HARMONIC ANALYSIS OF ANALYTICAL DATA FOR URANIUM IN LAKE SEDIMENTS IN THE GREAT BEAR LAKE REGION, N.W.T.

by

NIELS GREIG LUND, B.Sc.

A thesis submitted to the Faculty of Science in partial fulfilment of the requirements for the degree of Bachelor of Science (Honours)

Carleton University
Ottawa, Ontario
April, 1973

CONTENTS

ILLUSTRATIONS

ACKNOWLEDGMENTS

The author wishes to acknowledge the following people in alphabetical order: a) Dr. F.P. Agterberg, who provided mathematical advice and computer services; b) Dr. R.J. Allan, who was instrumental for the author's experience in geochemical exploration. His character, patience, enthusiasm, interest and advice will be lastingly appreciated and remembered; c) Dr. K. Bell, who acted as thesis supervisor and whose comments and advice were greatly appreciated; d) Dr. E.M. Cameron, who acted as external advisor and who suggested the thesis topic. He and Dr. Allan also provided the raw data and necessary technical services which were required for the presentation of the thesis; e) F. Chung, who provided the computer program for harmonic analysis and who was helpful in its interpretation; f) J.D. Hobbs, who supplied the computer contouring services and whose unselfish help was greatly appreciated.

The author would like to thank Dr. Allan, Dr. Bell and Dr. Cameron for their careful reading and criticism of this thesis.

ABSTRACT

Lake sediment samples were collected at a density of one sample per 25 sq. km. or 9 sq. mi. in a uraniferous area of the Great Bear Lake region, N.W.T.

The objective of the thesis was to treat analytical data for uranium in lake sediments by harmonic analysis. A two dimensional power spectrum showed several distinct peaks from which a number of sets of crest lines were constructed. The crest lines pass along uranium contour patterns and anomalous zones which are roughly parallel and equally spaced. The orientations of the various crest lines show a very good degree of directional similarity with postulated structural lineaments in the thesis area. The intersections of these crest lines account for most of the anomalous zones as do the intersections of various fault lineages account for the localization of known uranium deposits and mineralization. These similarities probably suggest that uranium deposits and mineralization within the Great Bear Lake region are controlled by regular structural features.

INTRODUCTION

The Bear Geological Province is a favourable area for the occurrence of uranium (Lang, 1958). The known occurrences and deposits occur along the western margin of the Province, and all are of the vein type. Because of this, the area is considered to be a metallogenic province for uranium (Lang et al., 1962). Figure 1 shows this in perspective with others that occur along the outer perimeter of the Shield and along two prominent geosynclines.

Within the Great Bear Lake region the known uranium deposits are controlled by lineaments and structural features associated with tectonism of late Aphebian age. The lineaments, many of which may be faults, are parallel and trend northeast (Ruzicka, 1971) and are separated by a regular spacing of 12 miles (Campbell, 1955).

Lang et al. (1962) and Ruzicka (1971) have postulated that the intersections of the northeasterly-trending lineaments with tectonically related fault and fracture systems of various directions (mainly southeast) provide structurally favourable loci for the localization of uranium deposits in the thesis area. Uranium deposits may also be closely associated with diabase dykes that fill some of the southeasterly fractures (Ruzicka, 1971).

Recently the Geological Survey of Canada undertook a large geochemical reconnaissance survey collecting lake sediment samples in the Bear-Slave Provinces (Allan et al., 1973). The thesis area covers approximately $\frac{1}{4}$ of the survey area and is situated in the Great Bear Lake region, N.W.T. (FIG.1).

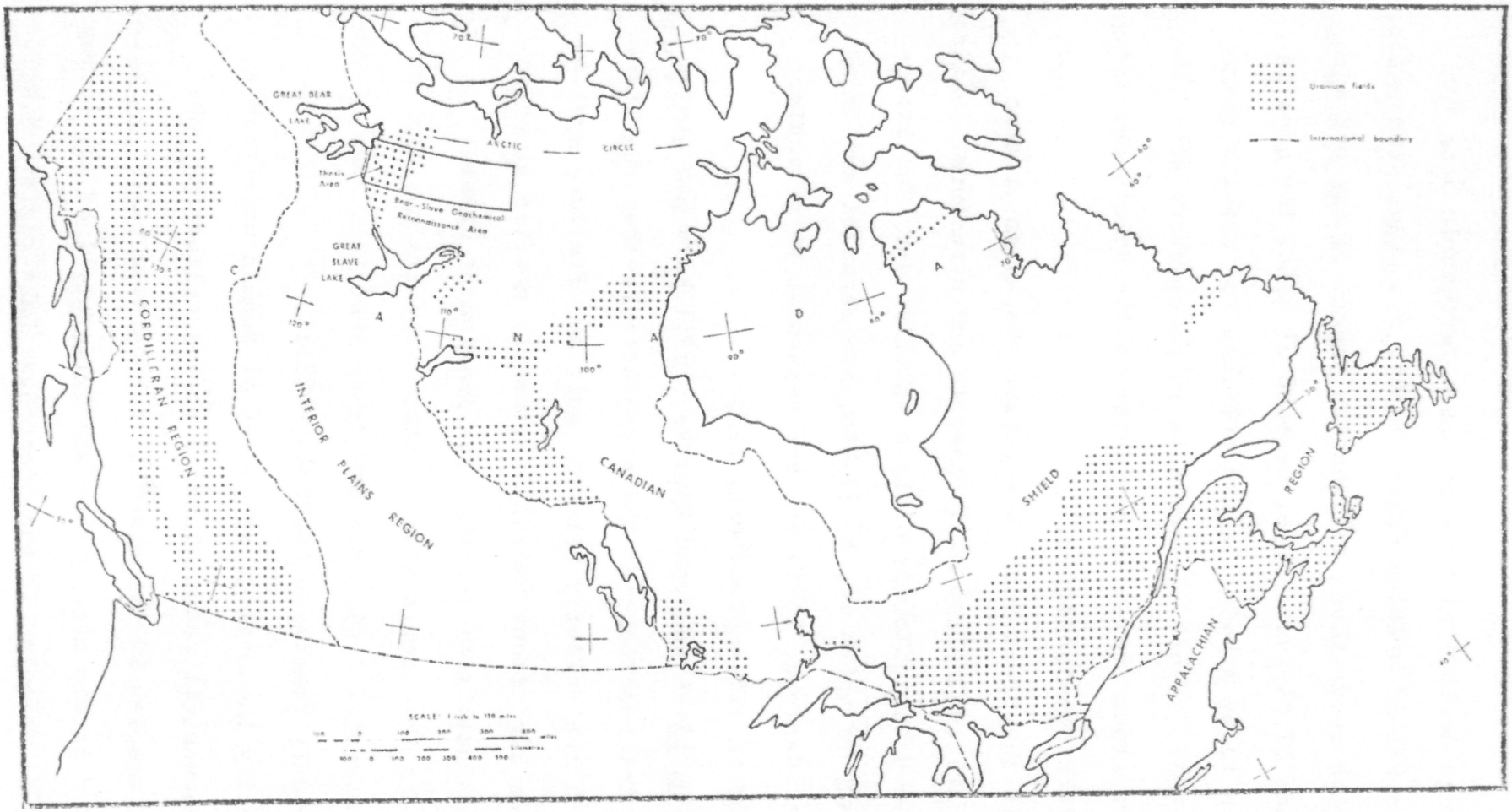

FIGURE 1. Area of geochemical survey and metallogenic map for uranium in Canada (modified from Lang, 1958).

The objective of the thesis is to mathematically analyse the uranium data in lake sediments by a method of harmonic analysis. The use of this approach is to detect one or more sets of parallel (or approximately parallel) lines in the analytical data. These lines, along which the anomalies tend to be clustered, are equally spaced (or nearly so). It is hoped that harmonic analysis will show whether or not the concept for uranium mineralization within the area is controlled by regular structural features.

GENERAL GEOLOGY

The Precambrian Bear Structural Province, situated along the western margin of the Archean Slave Province, is made up of Aphebian and Helikian sediments intruded by granitic plutons (FIG.2). The early Proterozoic sediments belong to what Hoffman (1973) calls the Coronation Geosyncline.

The oldest rocks are Aphebian sediments and volcanics of the Epworth and Snare Groups. Four phases are recognized: a pre-orogenic orthoquartzite-carbonate phase; a transitional euxinic-volcanic phase; an early syn-orogenic flysch phase; and a late syn-orogenic molasse phase (Hoffman, 1973; McGlynn and Fraser, 1972).

During the Hudsonian orogeny the Hepburn and Great Bear batholiths were emplaced. They are now separated by the 350 kilometer-long Wopmay fault (FIG.3). The Hepburn batholith comprises migmatites, mixed granitoid gneisses, granodiorite

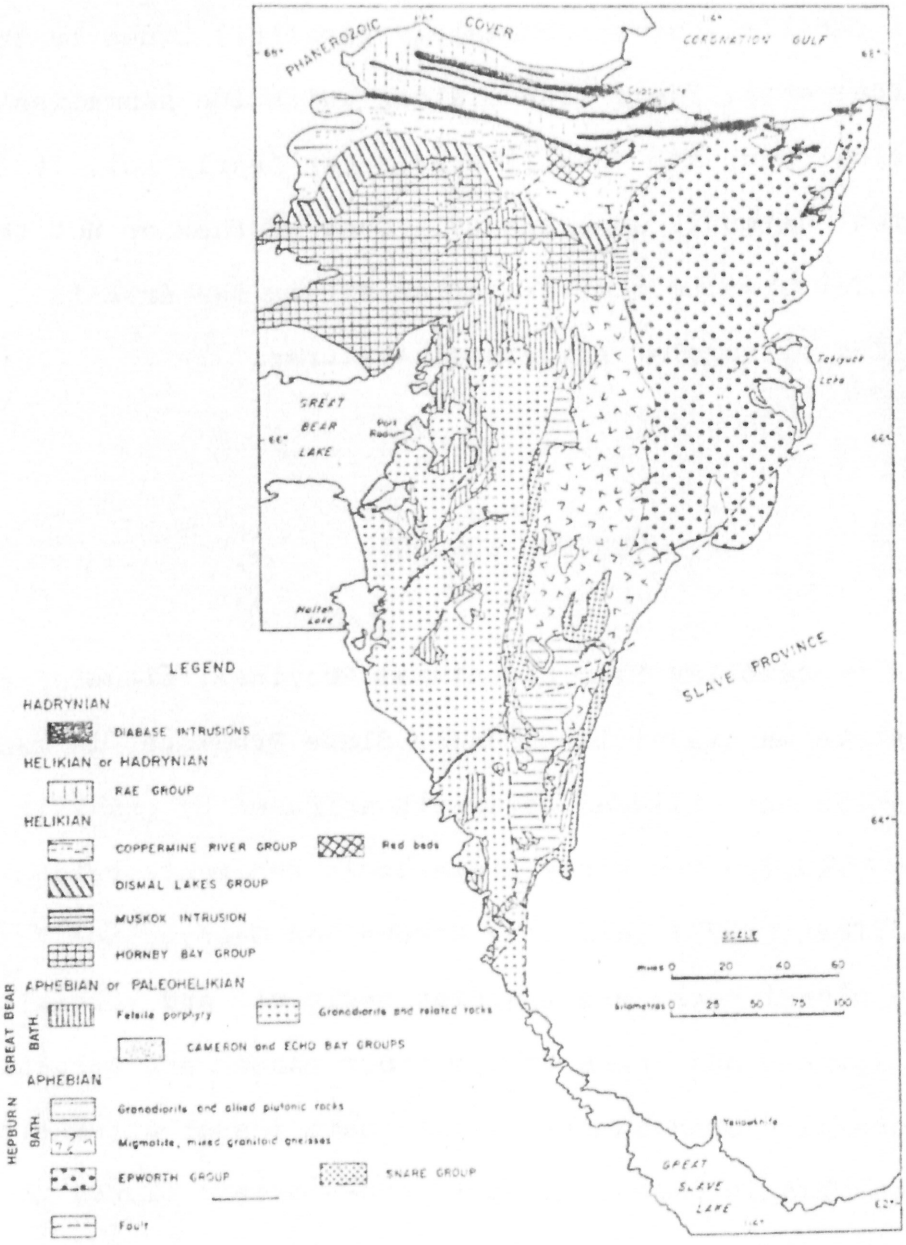

FIGURE 2. General Geology of the Bear Structural Province (from McGlynn and Fraser, 1972).

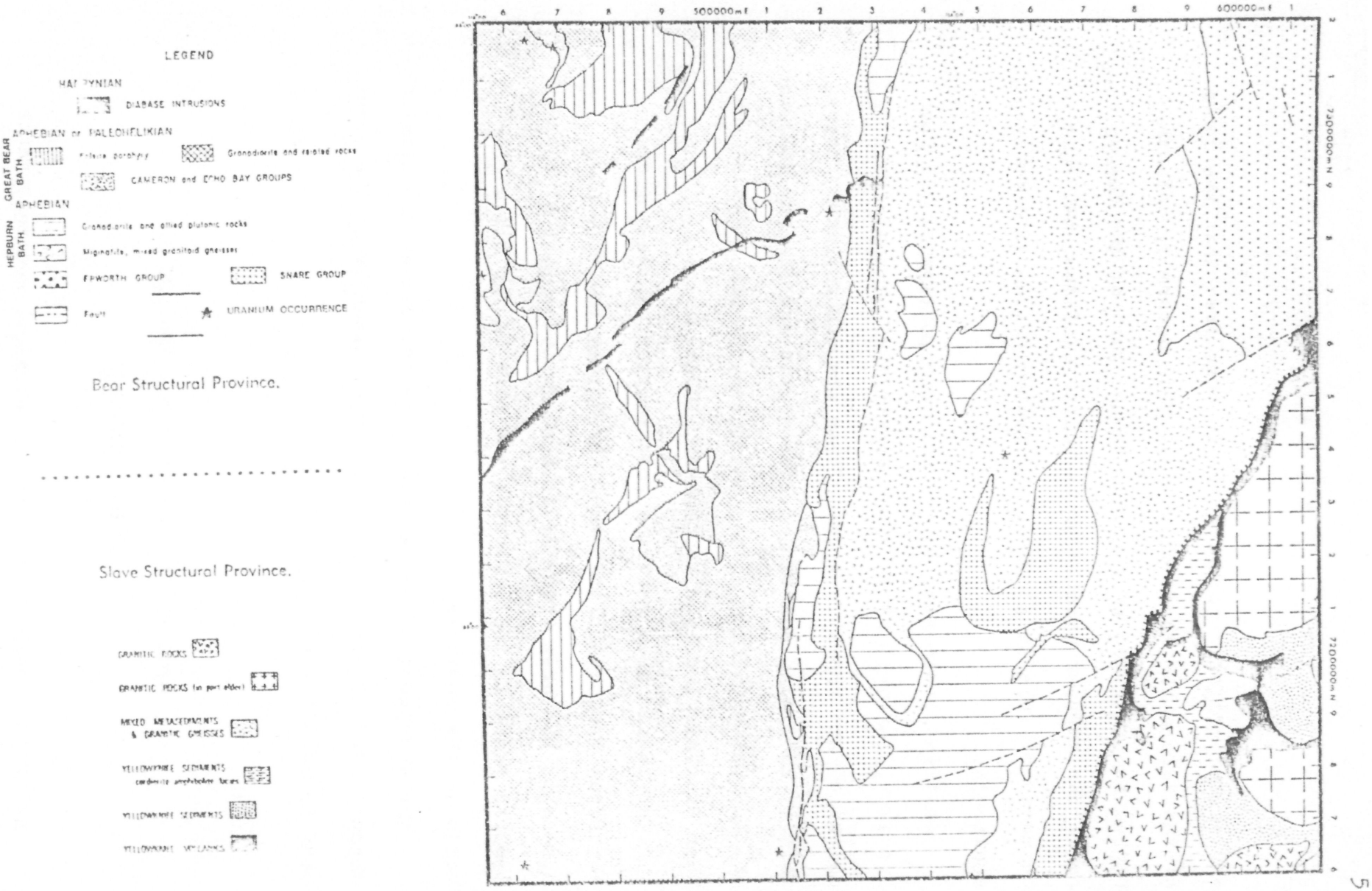

FIGURE 3. General geology of the thesis area.

and allied plutonic rocks. It is in this area that the rocks of the Coronation Geosyncline have been deformed, metamorphosed and intruded by granitic rocks. West of the Wopmay fault the younger Great Bear batholith (Hoffman, 1973) is composed of felsite porphyry and granodiorites with derived sediments.

Helikian sediments, in the northern portion of the Bear Province, consists of deformed quartzites, stromatolitic dolomites and basaltic lavas. These are unconformably overlain by Hadrynian quartzites, carbonates and shales. Helikian and Hadrynian diabase sheets and dykes cut all rocks of the Bear Province (McGlynn and Fraser, 1972).

The thesis area covers a good portion of the Hepburn and Great Bear batholiths with the Wopmay fault roughly bisecting the area (FIG.3). It also includes part of the Epworth Basin in the northeast and part of the Slave Province in the southeast.

The uranium geochemical anomalies as well as the uranium deposits and mineralization occur predominantly in the Great Bear batholith region (FIG.3).

GEOCHEMICAL EVIDENCE FOR THE USE OF HARMONIC ANALYSIS

After the completion of the geochemical reconnaissance survey, Allan and Cameron (1973) produced a uranium contour map that covers the thesis area (FIG.4). The anomalous

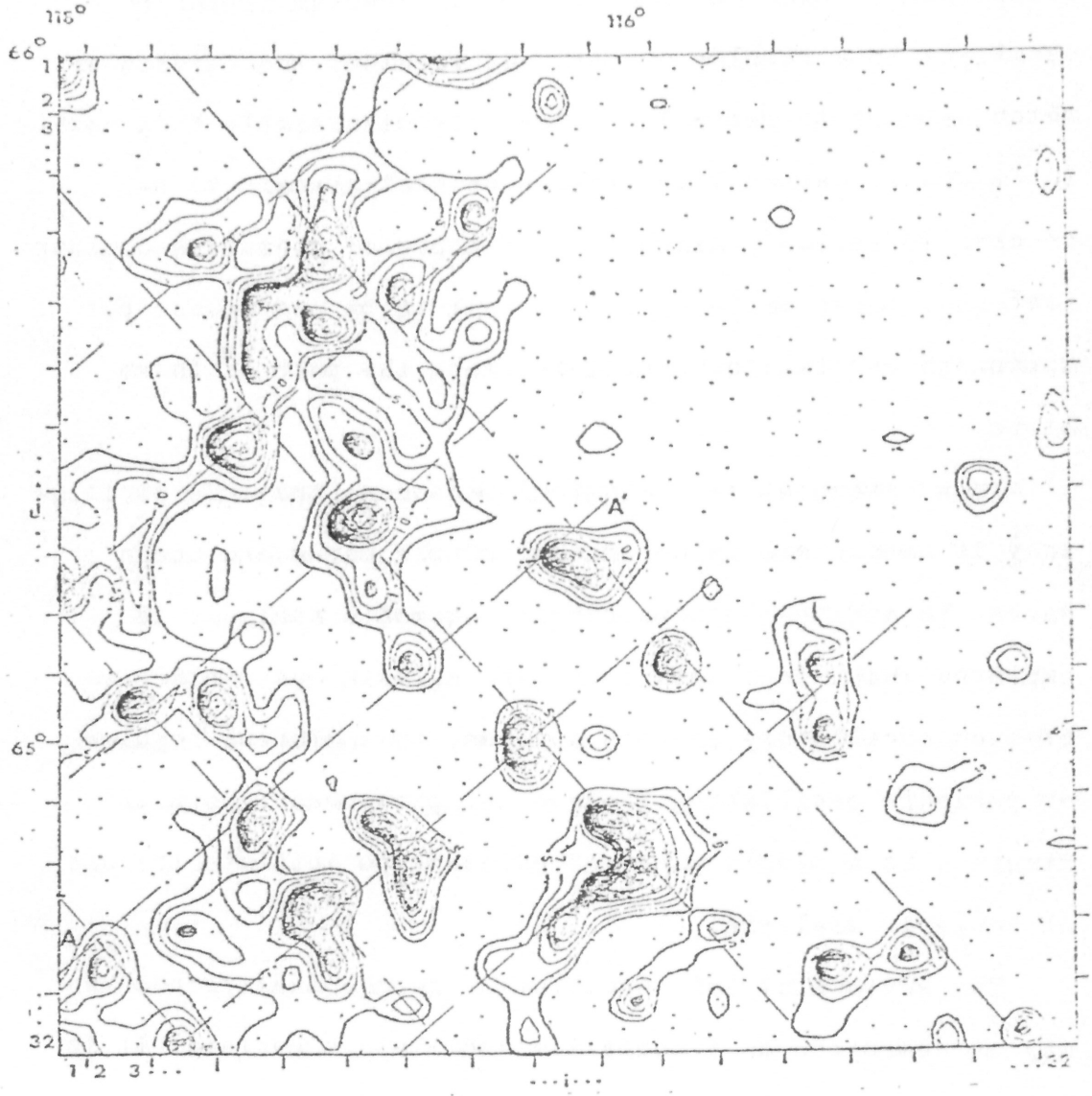

FIGURE 4. Contour map for uranium concentration in lake sediments, Great Bear Lake region, N.W.T. (Allan and Cameron, 1973). Shaded areas are anomalous zones of ≥ 15 ppm uranium and the dashed lines represent what appears to be regular or periodic alignments of anomalous zones (A-A', refer to FIG.5).

contour patterns ($\geq$ 15 ppm uranium) appear to show some degree of regular or periodic phenomena. That is, regional variations of high and low values for uranium appear to oscillate in a regular or periodic fashion: the surface of which appears to resemble the surface of a simple "egg box". In Figure 4, dashed lines represent what appears to be regular or periodic alignments of zones of anomalous contour patterns. These patterns do not seem to be continuous but appear to undulate or oscillate along the path of these lines.

Known examples of geological phenomena that are oscillatory in nature are folded rocks, ripple marks and ocean waves. To analyse such phenomena, harmonic analysis is employed which is a technique for analysis and synthesis of such oscillatory phenomena. Thus, the apparent regular or periodic oscillating geochemical phenomenon shown in Figure 4 is a simple piece of evidence to initiate the use of harmonic analysis.

The surface of this oscillating geochemical phenomenon may be described as a composite oscillatory surface. It is made up of two components, a periodic fluctuation and a random fluctuation (Harbaugh and Merriam, 1968). For example, Figure 5 shows a hypothetical cross section along A-A' of Figure 4, showing the random and periodic components.

When the composite oscillatory surface is contoured, as in Figure 4, the random fluctuation is reduced and the periodic component may become more evident. However, the periodic phenomena may not be obvious from this contour map

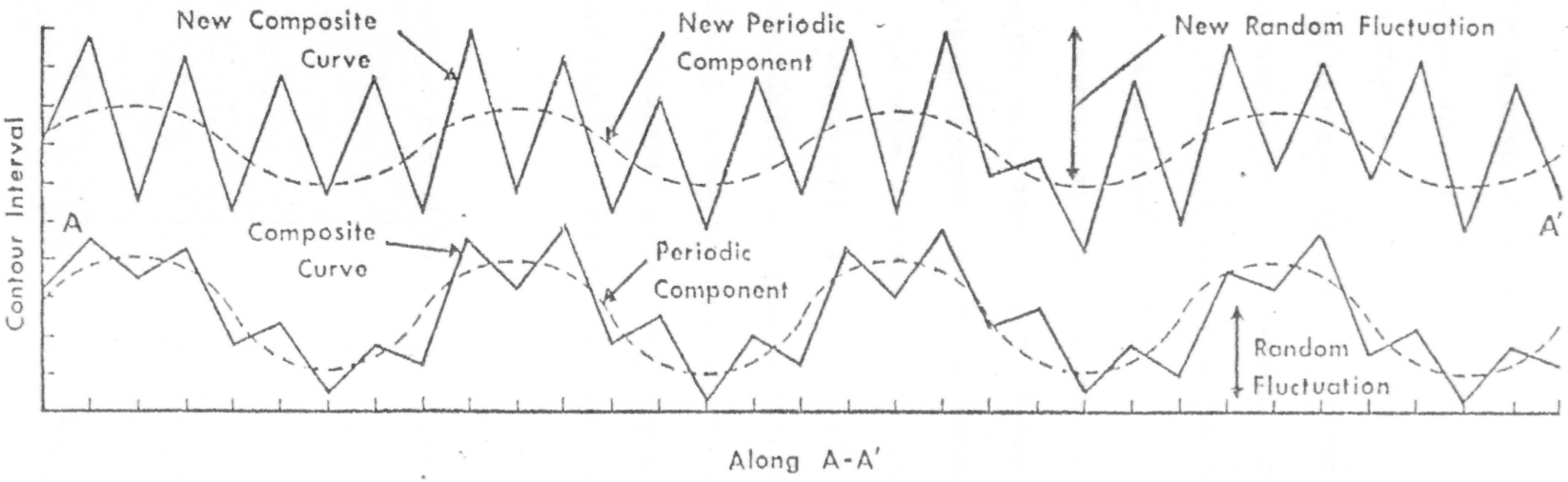

FIGURE 5. Hypothetical cross section of the composite oscillatory surface showing the random and periodic components.

and especially from the raw data. To demonstrate this, random numbers were added to the original data. The effect of this is shown in Figure 5 as the new composite curve. The underlying regional periodic phenomenon is still present, but the random fluctuation is more variable in amplitude than was the original random fluctuation. This has the effect of altering the original contour map, Figure 6a, to a new contour map with no periodic phenomena, Figure 6b.

If the random numbers chosen were too large, the apparent regional periodic trend would be completely destroyed. Alternatively, if the random numbers were too small there would be no appreciable change in the original map.

Thus, if a contour map shows no visible periodic phenomena and apparently resembles a random pattern, the application of harmonic analysis to the data will still bring out any hidden regional trend if it exists (see Appendix I).

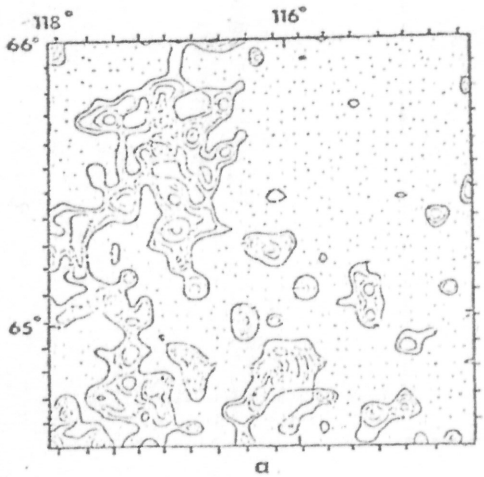

Original uranium contour map (FIG.4; Allan and Cameron, 1973).

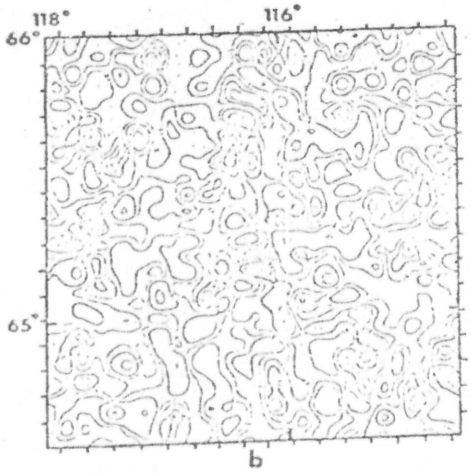

New uranium contour map with added random numbers.

FIGURE 6. Comparison between the original uranium contour map and the uranium contour map with the added random numbers.

HARMONIC ANALYSIS

(i) INTRODUCTION

The method of harmonic analysis used in this thesis follows similar procedures used by Agterberg and Fabbri (1972). It consists of coding a dot map (FIG.8) and calculating the two dimensional inverse complex Fourier transform which results in a power spectrum.

The term "spectrum" may bring to mind the separation of spectral colours in sunlight. This is accomplished by sunlight being dispersed through a prism resulting in characteristic wavelengths and spectral colours in the sunlight spectrum. An analogous result of this with respect to the mathematical method used is shown in Figure 7.

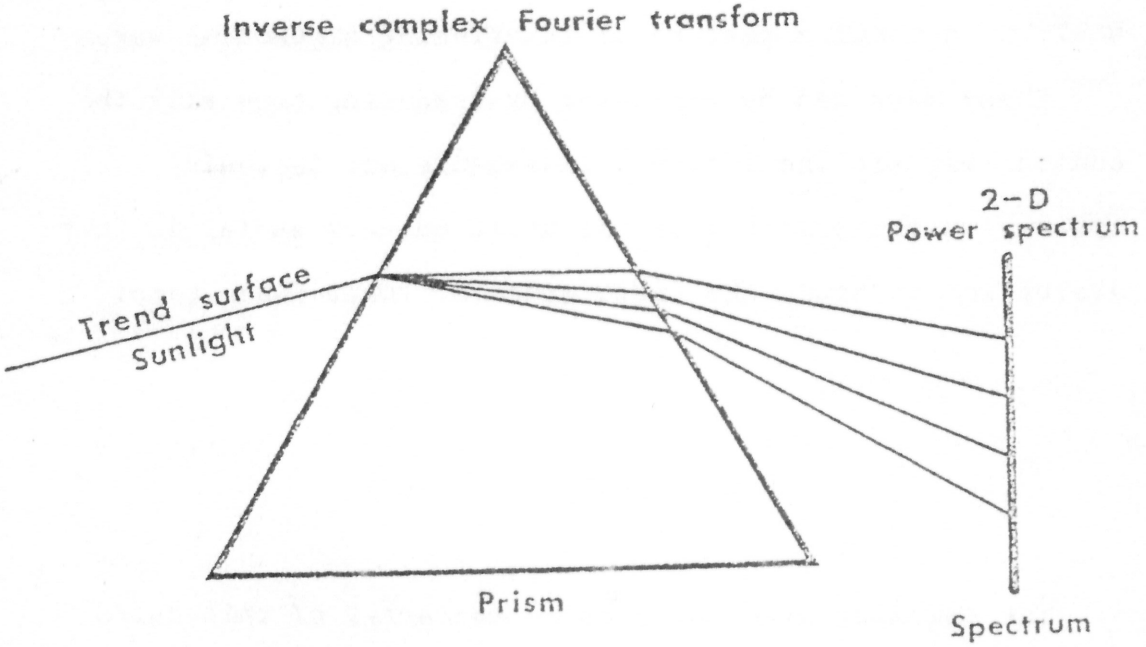

FIGURE 7. A diagram to illustrate analogous principles between dispersion of sunlight and the method of harmonic analysis used.

One might compare sunlight with the overall surface or trend surface for uranium content in lake sediments. Like sunlight, the uranium trend surface is a composite of its components.

The inverse Fourier transform may be compared to the properties of a prism. It disperses the trend surface into a power spectrum that distinguishes "signals" from "noise". The position of these signals or peaks may correspond to periodic regularities in the regional arrangement of the uranium content in lake sediments.

A chosen peak in the power spectrum gives rise to what is called a phase map. This map is a series of sinusoidal waves whose wavelength, amplitude and direction are dependent on the position and value of the peak chosen. If a collection of peaks were chosen the resulting phase map would be a complex pattern of interfering sinusoidal waves.

Phase maps can be evaluated by comparing them with the contour map and the inferred lineaments and tectonic systems in the thesis area. It would be very useful in this evaluation to study the crest lines of these phase maps.

(ii) NATURE OF THE DATA

The sampling area conforms to the array of unit cells defined by the Universal Transverse Mercator projection (U.T.M.) on a scale of 1:250,000. Each one of these 10x10 km. unit cells is divided into four 5x5 km. cells each

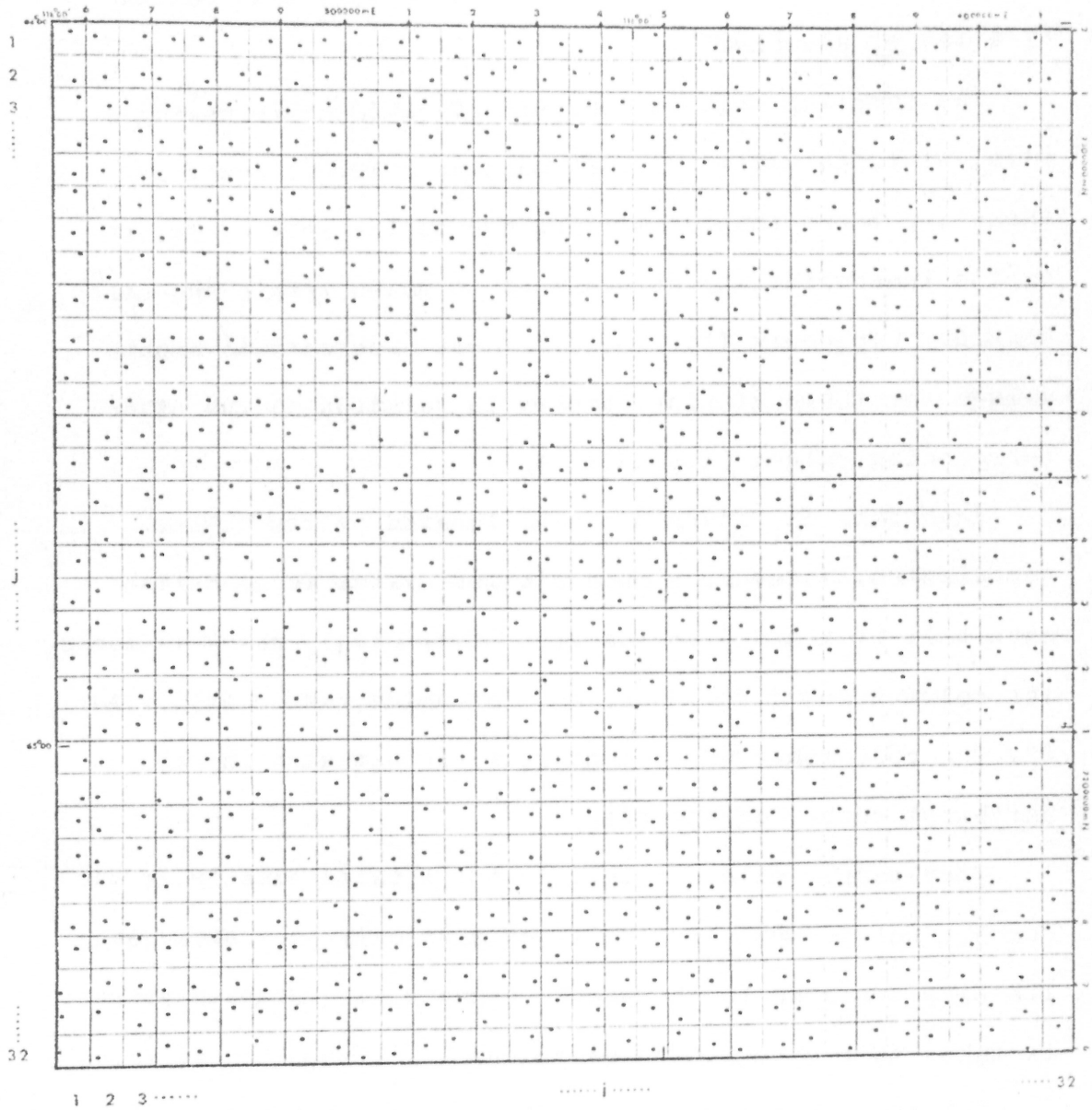

FIGURE 8. Lake sediment sample sites, Great Bear Lake region, N.W.T. 5x5 sq. km. cells based on the U.T.M. system. Cells are located by reading i and j coordinates.

containing one lake sediment sample (FIG.8). The sample density of one sample per 25 sq. km. or 9 sq. mi., in an area of continuous permafrost, complies with that defined by Allan et al. (1972).

The sampling grid is composed of 32x32 cells making a total of 1,024 cells or 1,024 samples (FIG.8). However, there are three samples missing due to the lack of lakes or the inacessibility of sediment in lakes within the cell boundary (Appendix II; FIG.8). It was necessary to assume values for these missing samples in relation to the other surrounding values (Appendix III).

Each cell in Figure 8 can be located by its U.T.M. coordinates. However, a much simpler system is to define each cell by i and j coordinates, i.e. (i,j), where i stands for columns and j for rows, each of which varies from 1 to 32. The coordinate or element (1,1) is situated in the northwest corner of the grid.

Each sample within a cell is not located exactly in the center, but because each cell contains only one sample and its size conforms to the sample density, the uranium value is taken to represent the whole cell.

All the samples were collected by burrowing an auger into the lake bottom sediment. Helicopters were used to reach the sample sites. The depth of samples in lakes averaged approximately 5 feet and ranged from 3 to 8 feet. The sediment was placed into water-proof bags, and after being air dried were shipped to Ottawa for immediate sample preparation and chemical analysis.

The samples were sieved (< 250 mesh), then analysed for uranium content by a fluorescence method (Smith and Lynch, 1969).

(iii) METHOD OF HARMONIC ANALYSIS

To mathematically describe the uranium trend surface appropriate variables must be established. The uranium content in lake sediments represents a dependent variable, z, which becomes a function of two independent variables, i and j which represents easterly and southerly directions respectively.

These i and j variables correspond to the i and j coordinates given in Figure 8 and Appendix II and III. Every z has a uranium value U(i,j), and therefore z=U(i,j).

The elementary or observed array of gridded data U(i,j) is a square array with i and j varying from 1 to 32:

$$\begin{matrix} U_{1,1} & \cdots\cdots & U_{1,32} \\ \vdots & & \vdots \\ U_{32,1} & \cdots\cdots & U_{32,32} \end{matrix}$$

The average value was subtracted from each U(i,j) value giving rise to a basic array of elements X(i,j) that are corrected for the mean.

The inverse complex Fourier transform was then computed by the general equation:

$$A(p,q)=1/n^2\sum_{j=1}^{n}\sum_{i=1}^{n}X(i,j)\exp(-2\pi I(ip/n+jq/n)) \quad \ldots\ldots\ldots(1)$$

where $I=\sqrt{-1}$ and $n=32$.

From this equation A(p,q) consists of a real part, Re(A(p,q)), and an imaginary part, Im(A(p,q)). By computing the square of the amplitude its phase is eliminated:

$$P'(p,q)=Re^2(A(p,q)) + Im^2(A(p,q)) \quad \ldots\ldots\ldots\ldots\ldots\ldots(2)$$

Every value P'(p,q) was standardized by multiplication by the factor $F=n^2/s^2$ where s^2 is the mean square of the array X(i,j). The resulting (32x32) array of P(p,q) values is the power spectrum which is symmetrical about the origin P(0,0). Therefore, only half of it is represented in map form (FIG.9). Every P(p,q) value can be located in Figure 9 by using the scales on the bottom (for p values) and sides (for q values).

Each value P(p,q) in the power spectrum is related to the amplitude for a single sine wave fitted to the data in the dot map (FIG.8). The axis of this wave is perpendicular to the line joining P(p,q) to the origin P(0,0). The distance between the two points determines the period of the wave which is measured by rotating the period scale about the origin.

Our interest is now directed to peaks some distance

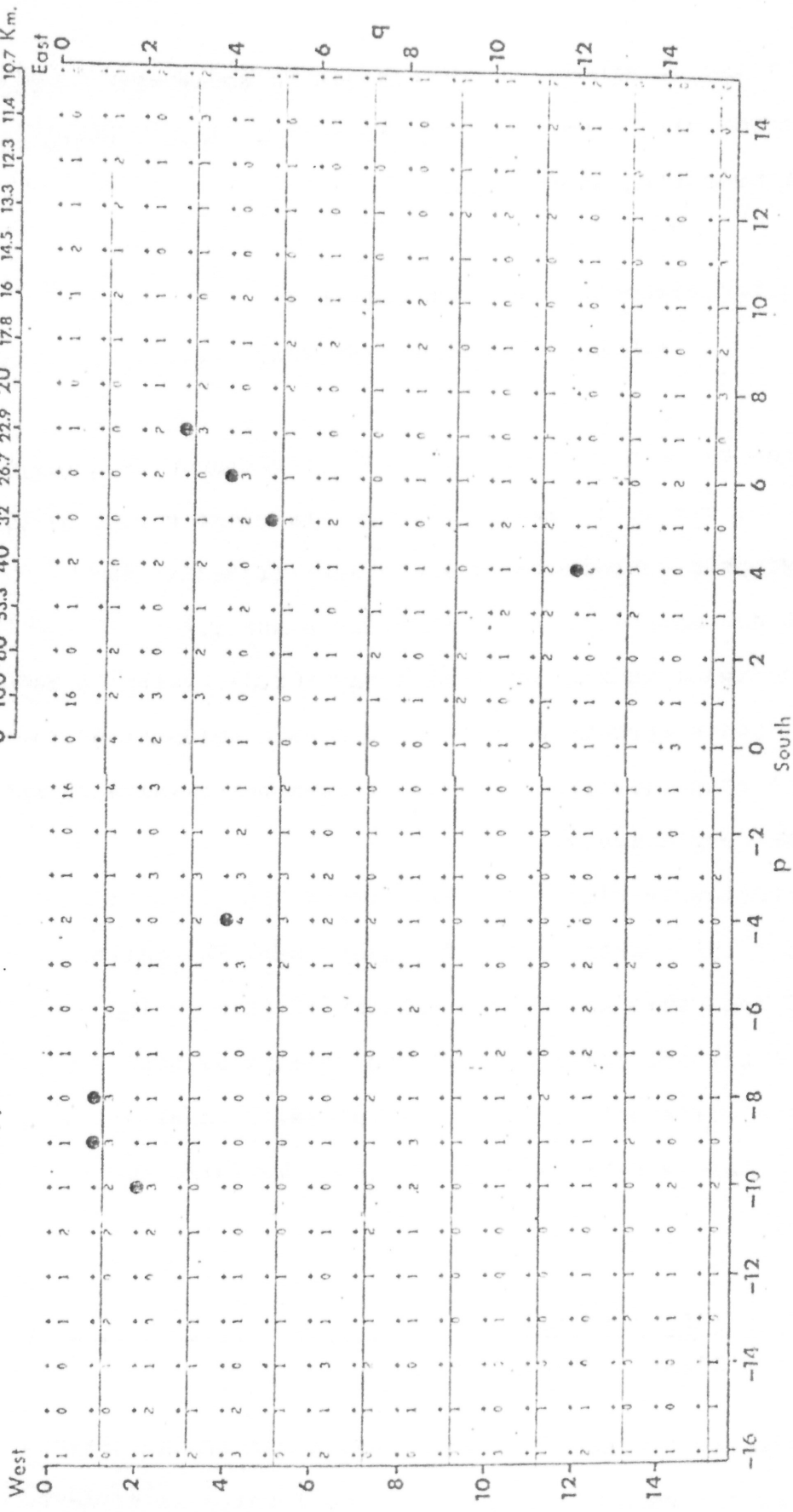

FIGURE 9. Power spectrum for uranium content in lake sediments, Great Bear Lake region, N.W.T. The large dots denote $\Gamma(p,q)$ values chosen for the construction of phase maps.

away from the origin which corresponds to waves with periods of approximately 30 km. or less. From these points phase maps can be constructed as follows:

$$X'(p,q:u,v)=Re(A(p,q))\cos 2\pi(pu/n+qv/n) - Im(A(p,q))\sin 2\pi(pu/n+qv/n) \quad \ldots\ldots\ldots\ldots\ldots (3)$$

It can be seen that equation (3) corresponds to a single term of the complete complex Fourier transform A(p,q) of (1). The geographic coordinates u and v were fitted to the original dot map (FIG.8) for specific p and q.

Where i=j=1 in the original array X(i,j), u=v=0 in the new coordinate system. When i and j denote columns and rows of X(i,j) respectively, the u and v axes point eastward and southward respectively.

As previously stated, several peaks P(p,q) could be chosen for the construction of a phase map. The pattern produced from this would be a pattern of interfering sine waves. If several peaks were chosen, the phase maps X'(u,v) would have different high and low values. Because of this, the phase maps were standardized using the following equation:

$$X(u,v)=\frac{X'(u,v)+|X'min|}{X'max+|X'min|} \quad \ldots\ldots\ldots\ldots\ldots\ldots\ldots\ldots\ldots (4)$$

where X'min is the smallest value and X'max is the largest value. The new range of X(u,v) is 0 to 1 which is divided into seven segments, each of which has a symbol for easy

graphical recognition (see FIG.10a-e). These symbols, of increasing value, are as follows: b,-,b,+,b,X,X where b is a blank. Crests of waves or interfering waves are recognized by bands of X-signs.

PHASE MAPS FOR URANIUM CONTENT IN LAKE SEDIMENTS

The most important phase maps follow. These are based on peaks selected from the power spectrum in Figure 9. The areas of these maps (FIG.10a-e) are the same as the area for the uranium contour map shown in Figure 4. Each phase map description is identified by the figure number and the set of points used. Other phase maps that show patterns from several peaks are shown in Appendix IV.

FIGURE 10a. N-S set: P(-9,1)=3.

The crest lines are in a N-S direction with a wavelength of approximately 17 km.

FIGURE 10b. NW-SE set: P(-4,4)=4.

The crest lines of this phase map are directed in a NW-SE direction with a wavelength of approximately 28 km. They seem to best fit postulated southeasterly trending fault, fracture and diabase dyke systems in the thesis area.

FIGURE 10c. E-W set: P(4,12)=4.

The wave pattern is not directly east-west but is directed more northerly. The wavelength is approximately 12.5 km.

FIGURE 10d. NE-SW set: P(6,4)=3.

The crest lines are in a NE-SW direction with a wavelength of approximately 21.5 km. or 12.9 mi. They seem to best fit theoretical northeasterly trending lineaments in the thesis area.

FIGURE 10e. NE-SW-NW-SE set: P(-4,4)=4; P(6,4)=3; P(4,12)=4; P(-9,1)=3.

The peaks chosen are the major signals in the power spectrum (FIG.9). The crest lines no longer form lines but form crest modes. A three dimensional view of this phase map appears to resemble the surface of a simple "egg box".

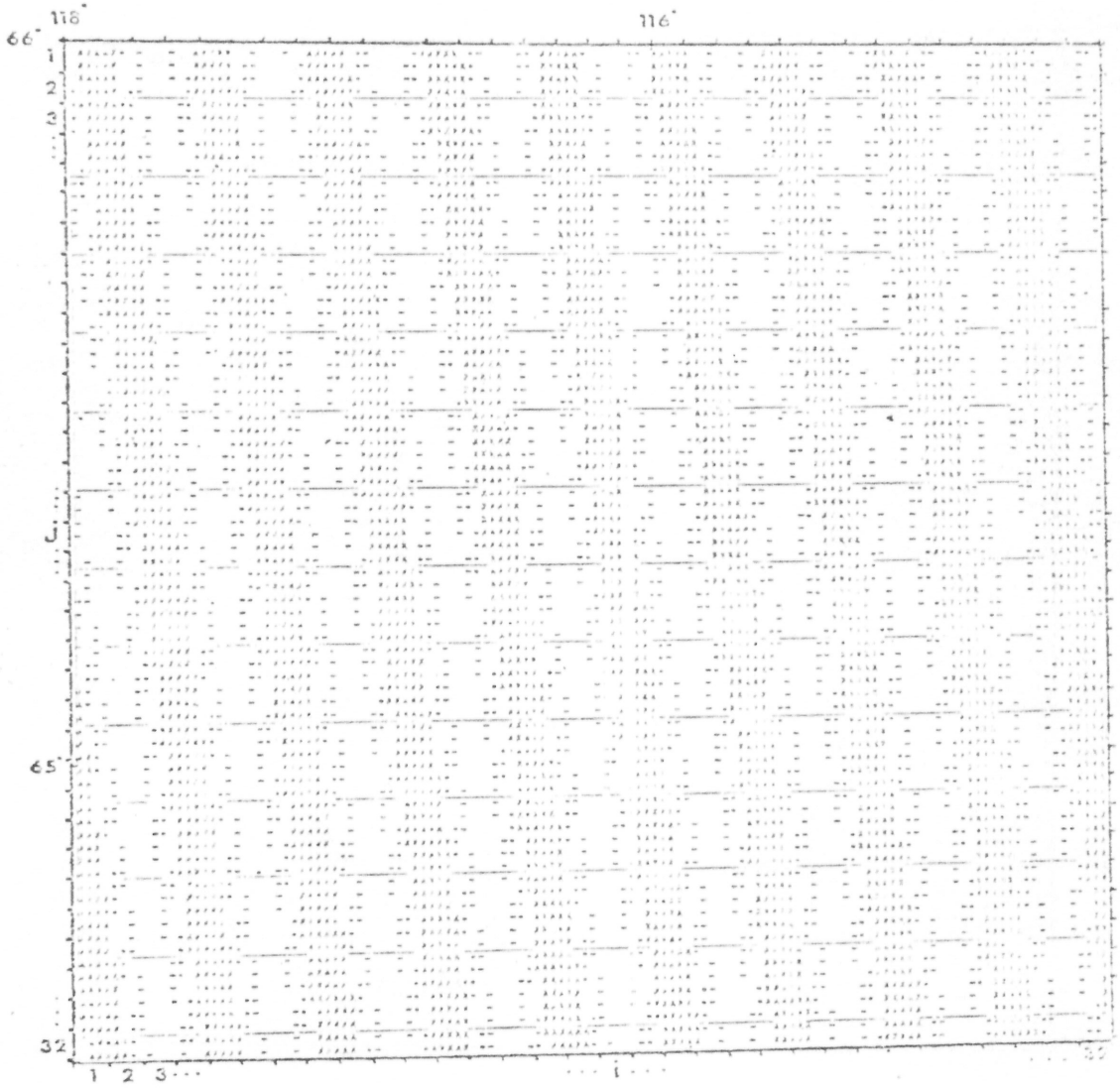

FIGURE 10a. Phase map constructed from peak P(-9,1).

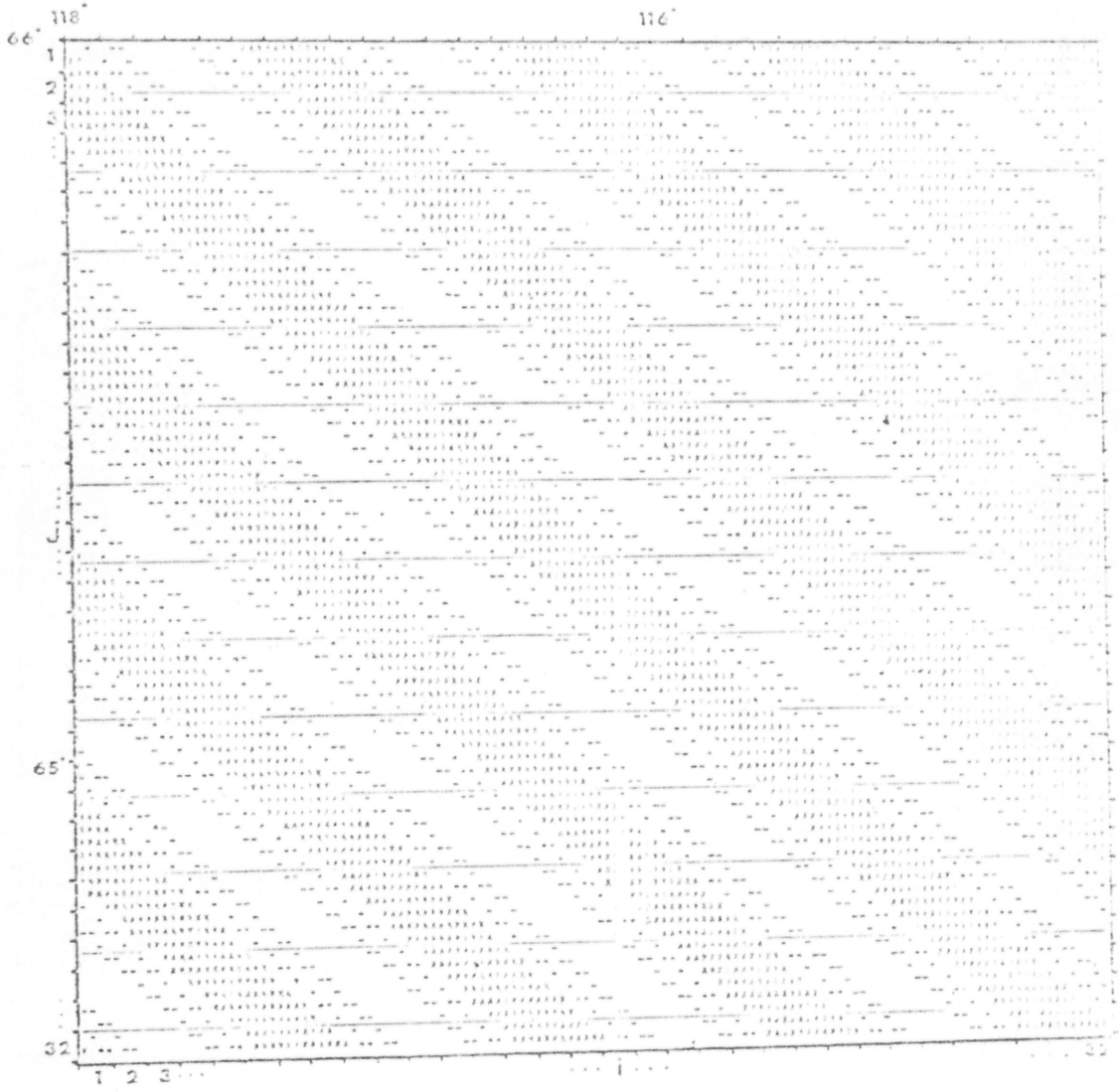

FIGURE 10b. Phase map constructed from peak P(-4,4).

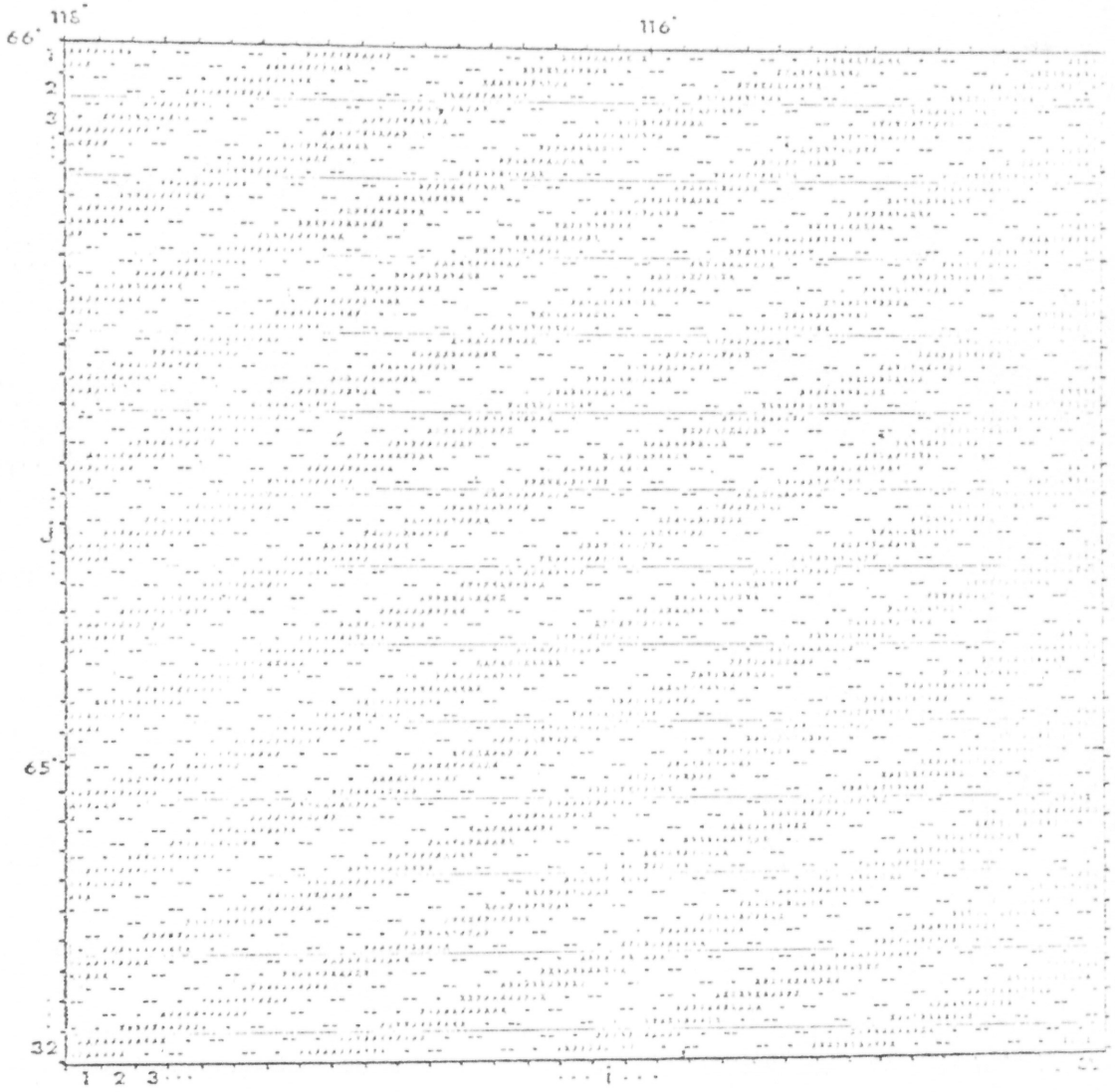

FIGURE 10c. Phase map constructed from peak P(4,12).

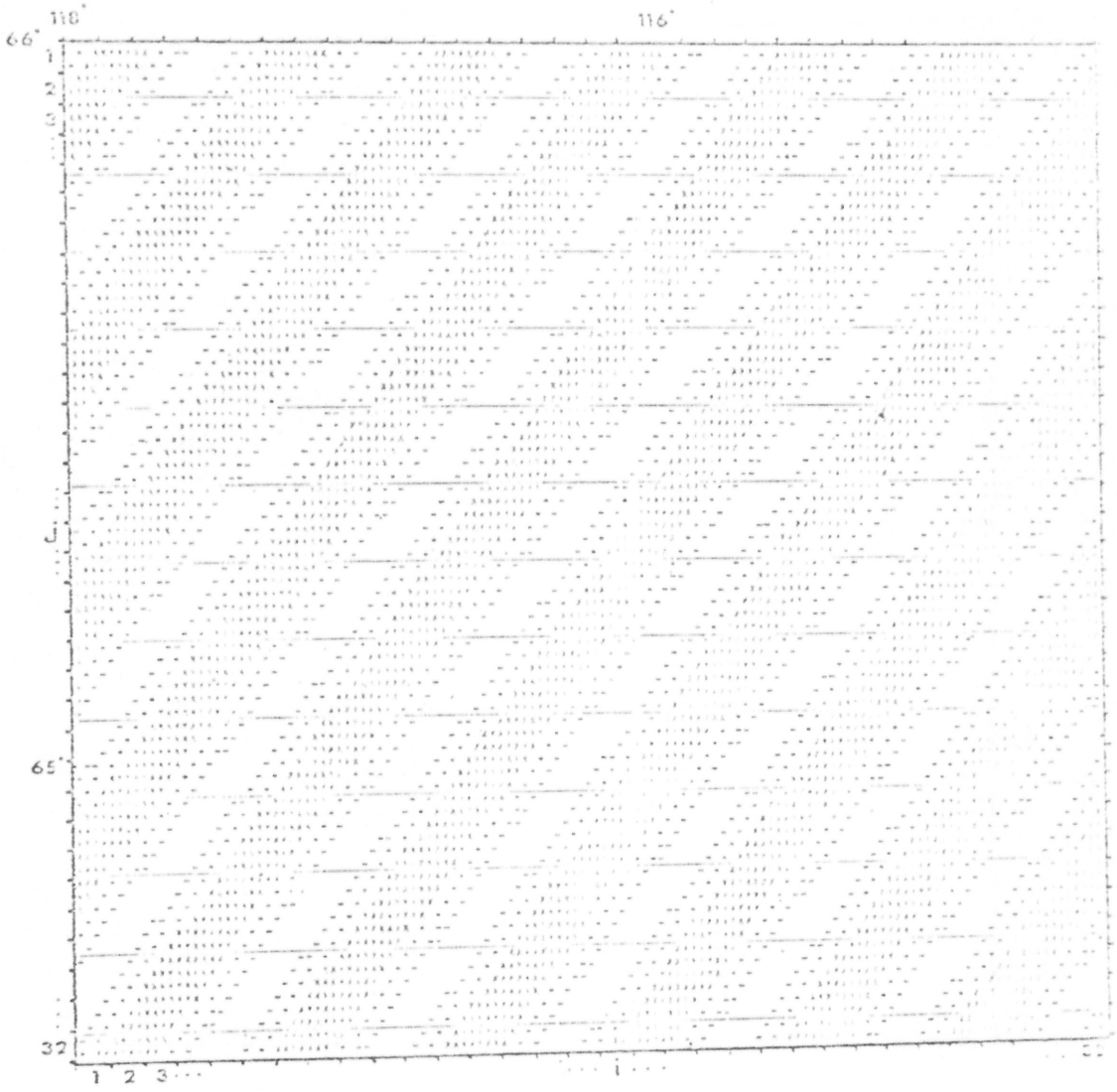

FIGURE 10d. Phase map constructed from peak $P(\epsilon,-)$.

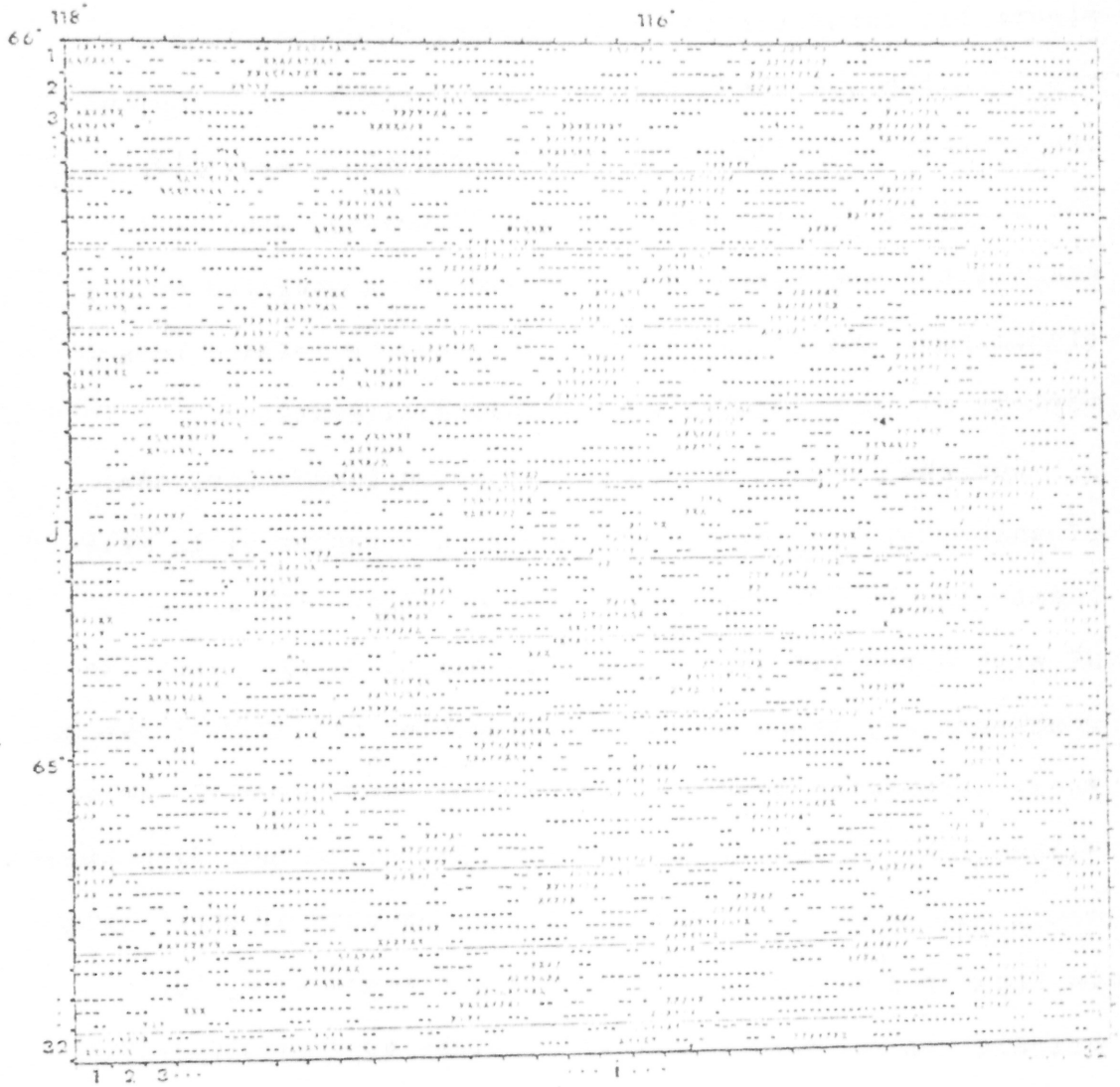

FIGURE 10e. Phase map constructed from peaks P(-4,-7), P(6,4), P(4,12) and P(-9,1).

GEOLOGICAL INTERPRETATION OF ANALYSIS

Figures 10a-e show that the pattern of uranium distribution follows or aligns along various parallel and equally spaced crest lines of the various phase maps. As shown in Figure 11, these various crest lines, belonging to a N-S set (FIG.10a), a NW-SE set (FIG.10b), a E-W set (FIG.10c) and a NE-SW set (FIG.10d), can be related to anomalies in the original uranium map (FIG.4). Of course, some of the crest lines and parts of others are not associated with a significant amount of uranium. This may be related to a variety of more complex geological considerations.

Ruzicka (1971) mentions NE trending lineaments, many of which may be faults, with a regular spacing of 12 miles (Campbell, 1955). The crest lines of Figure 10d are also NE with a regular spacing of 12.9 miles. He also mentions southeasterly trending faults, fractures and diabase dykes. These orientations are similar to the NW-SE crest lines of Figure 10b. He further mentions faults of various directions which may correspond to the N-S and E-W sets of crest lines in Figures 10a and 10c. In almost all cases then, the orientation of the various crest lines approximate directions of hypothesised structural lineaments. The various crest lines and fault systems show a very good degree of directional similarity.

It has been stated earlier that the structurally favourable loci for uranium deposits occur at the intersections of the various fault lineages, which correspond to the various crest lines, and therefore these too may show directional similarity. If this were true, then all

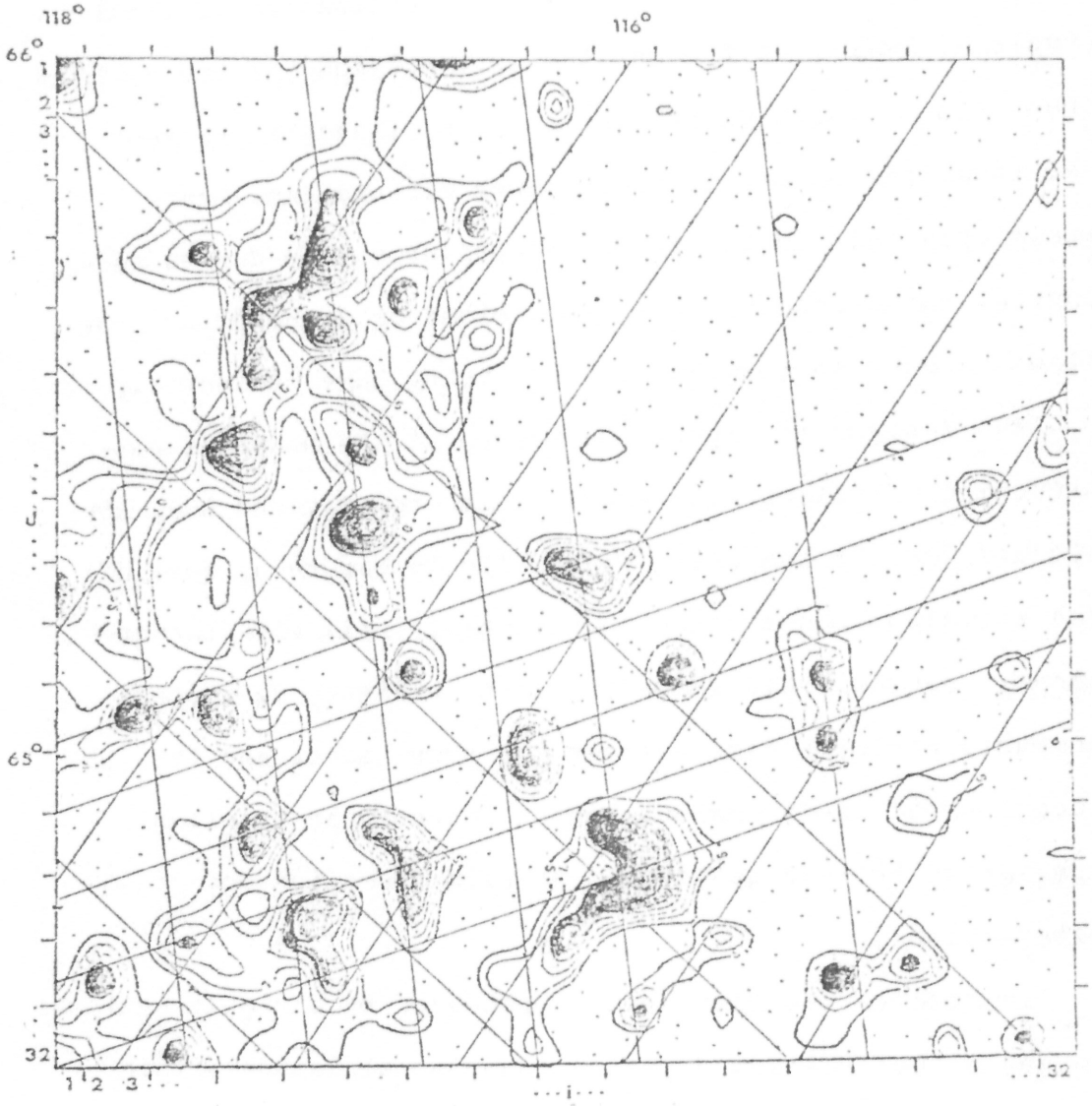

FIGURE 11. Selected crest lines showing how they correspond to uranium contour patterns and anomalous zones (shaded areas ≥ 15 ppm uranium).

loci, as shown in Figure 11, should have abnormal abundances of uranium. Just as the intersections of fault lineages are thought to control the localization of uranium (Ruzicka, 1971), so too may the intersections of the various crest lines, which correspond to these lineages, reflect the localization of anomalous zones for uranium. Overwhelmingly this is the case, exceptions may be due to geological variations so far undetermined or to sampling problems related to regional surveys using lake sediments.

The X-signs in Figure 10e represent the modes of construction of interacting crest lines from Figures 10a, 10b, 10c and 10d. By comparing Figure 10e to Figure 4, most of the anomalous zones coincide reasonably well with the crest modes. However, this is better seen in Figure 11 where a comparison can be made between the crest modes and the locations of the anomalous zones. There is an excellent similarity between control of uranium anomalies and crest interactions.

Therefore, the similarities produced by harmonic analysis suggests that uranium deposits and mineralization within the Great Bear Lake region are controlled by regular structural features which are related to the geotectonic evolution of this northwestern part of the Canadian Shield.

CONCLUSIONS

Harmonic analysis of geochemical data has shown that the trend surface or pattern of uranium content in lake sediments in the Great Bear Lake region is somewhat regular or periodic in nature. The use of this mathematical technique implies that there are regular structural features controlling the localization of uranium mineralization on a regional scale in this known uraniferous province.

The dominant structural features in the area are faults, fractures and diabase dykes trending in various directions. The regular NE-SW and NW-SE patterns of mathematically derived crest lines for uranium show directional similarities with NE and SE fault and fracture systems. The intersections of these fault and fracture systems have been postulated as areas of abnormal abundances of uranium. The intersections of the regular patterns of crest lines for uranium tends to confirm this geotectonic control of abnormal uranium levels. The implication is that uranium deposits and mineralization in the Great Bear Lake region are controlled by regular mathematically predictable structural features.

These conclusions could result in a format for uranium exploration using geomathematical interpretive techniques for areas where periodicity of uranium anomalies can be established.

REFERENCES

Agterberg, F.P. and Fabbri, A.G.

1972: Harmonic analysis of copper and gold occurrences in the Abitibi area of the Canadian Shield; Proc. Tenth Symposium Application of Computers in Mineral Industry, Johnnesburg, South Africa, (in press).

Allan, R.J. and (in part) Lynch, J.J. and Lund, N.G.

1972: Regional geochemical exploration in the Coppermine River area, District of Mackenzie; a feasibility study in permafrost terrain; Geol. Surv. Can., Paper 71-33.

Allan, R.J. and Cameron, E.M.

1973: Uranium in lake sediments; Geol. Surv. Can., Map 9-1972.

Allan, R.J., Cameron, E.M. and Durham, C.C.

1973: Reconnaissance geochemistry using lake sediments of a 36,000 square mile area of the northwestern Canadian Shield (Operation Bear-Slave, 1972); Geol. Surv. Can., Paper 72-50.

Campbell, D.D.

1955: Geology of the pitchblende deposits of Port Radium, Great Bear Lake, N.W.T.; unpubl. Ph.D. thesis; Calif. Inst. Technol.

Harbaugh, J.W. and Merriam, D.F.

1968: Computer applications in stratigraphic analysis; John Wiley & Sons, Inc.

Hoffman, P.

1973: Evolution of an early Proterozoic continental margin: the Coronation geosyncline and associated aulacogens of the northwestern Canadian Shield; Geol. Surv. Can. (in press).

Lang, A.H.

1958: Metallogenic map, uranium in Canada; Geol. Surv. Can., Map 1045-M1.

Lang, A.H., Griffith, J.W. and Steacy, H.R.

1962: Canadian deposits of uranium and thorium; Geol. Surv. Can., Econ. Ser. No. 16 (second edition).

McGlynn, J.C. and Fraser, J.A.

1972: Archean and Proterozoic geology of the Yellowknife and Great Bear areas, Northwest Territories, Field Excursion A27; International Geological Congress, session 24.

Ruzicka, V.

1971: Geological comparison between East European and Canadian uranium deposits; Geol. Surv. Can., Paper 70-48.

Smith, A.Y. and Lynch, J.J.

1969: Field and laboratory methods used by the Geological Survey of Canada in geochemical surveys, No. 11. Uranium in soil, stream sediment and water; Geol. Surv. Can., Paper 69-40.

APPENDIX I

A NEW POWER SPECTRUM

To show that the method of harmonic analysis (the inverse complex Fourier transform) will bring out any hidden trends from the random pattern of the uranium contour map in Figure 6b, a new power spectrum was computed for uranium values to which were added random numbers (FIG.6b). For the new periodic component to be similar to the original periodic component, the signals in the new power spectrum (FIG.I-1) should have similar coordinates and values for the signals in the original power spectrum. In Figure I-1 the four major signal areas in the new power spectrum correspond reasonably well with the signal areas in the original power spectrum (FIG.9). This demonstrates that the data will show regional periodicity, whether it can be recognized visibly or not. This is the concept and purpose of harmonic analysis.

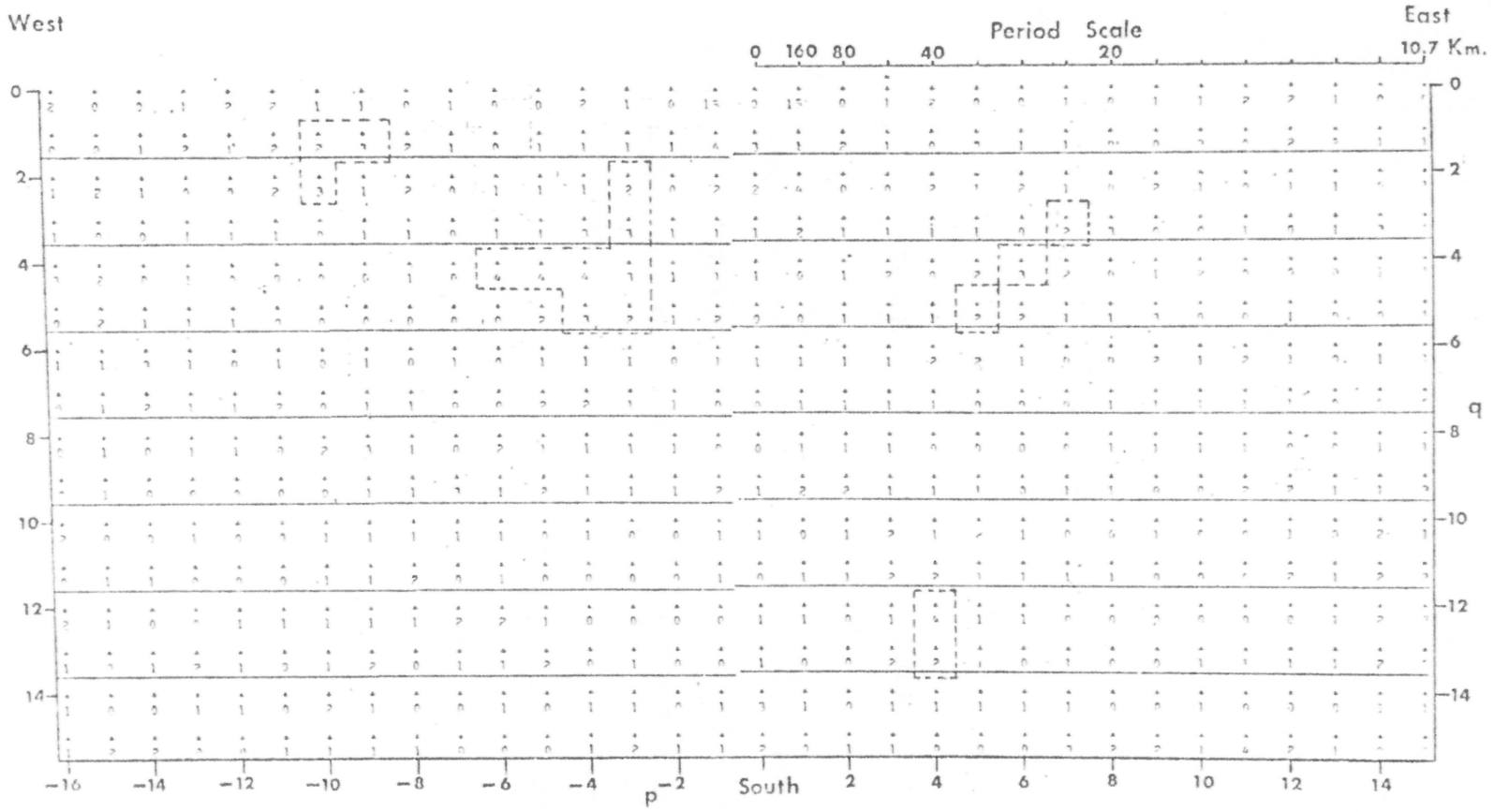

FIGURE I-1 Diagram showing the new power spectrum for uranium plus random numbers. Dashed lines show signals from original power spectrum (FIG.9).

APPENDIX II

TABLE OF SAMPLE SITE NUMBERS

The sample numbers are arranged to correspond to the sample site locations in Figure 8. To locate the sample number for a dot in Figure 8, read the i and j cell coordinate and then locate the same i and j coordinate in the tables that follow.

1	2115	2116	2121	2122	2128	2129	2130	2066	2067	2068	2071	2072	2233	2232	2229	2226
2	2114	2117	2120	2123	2127	2132	2131	2064	2063	2069	2070	2073	2234	2231	2230	2225
3	2113	2118	2119	2124	2125	2136	2133	2065	2062	2076	2075	2074	2236	2235	2224	2243
·	2111	2110	2109	2108	2107	2106	2105	2061	2060	2077	2059	2058	2238	2237	2223	2242
·	2173	2179	2107	2103	2190	2103	2104	2075	2078	2056	2057	2053	2239	2240	2222	2241
·	2177	2180	2186	2189	2191	2102	2134	2080	2081	2055	2054	2052	2219	2220	2221	2252
	2176	2182	2183	2185	2192	2101	2135	2085	2084	2082	2083	2051	2218	2217	2216	2251
	2175	2174	2184	2194	2193	2100	2136	2086	2087	2088	2089	2050	2213	2214	2215	2250
	2172	2173	2196	2195	2159	2150	2099	2177	2130	2139	2140	2049	2212	2253	2256	4250
	2170	2171	2163	2161	2160	2157	2098	2097	2096	2141	2142	2048	2211	2255	2257	4249
	2168	2165	2164	2162	2156	2155	2154	2153	2095	2094	2143	2047	2210	2259	2258	4248
	2167	2166	2155	2197	2198	2199	2200	2152	2093	2092	2144	2045	2209	2260	2261	4247
·	2013	2012	2021	2022	2023	2024	2025	2201	2151	2091	2145	2046	2208	2262	2263	4246
·	2017	2029	2030	2029	2028	2027	2026	2202	2203	2150	2090	6010	2207	2265	2264	4245
·	2016	2031	2033	2034	2035	2036	2039	2039	2042	2043	2149	2148	2206	4244	4243	4242
j	2032	2015	2012	2009	2000	2000	2037	2040	2041	2044	2204	2147	2205	4193	4195	4196
	2015	2014	2011	2010	2007	2005	2004	2003	2002	2001	6005	2146	6009	6003	6002	4197
·	4010	4009	4008	4007	4006	4005	4004	4003	4002	4001	6006	6011	6008	45	44	45
·	4011	4012	4034	4035	4036	4037	4038	4039	4042	4043	6012	6007	0[1]	92	91	90
	4032	4031	4030	4027	4026	4023	4022	4040	4041	4044	6013	178	177	176	6000	89
	4013	4033	4029	4028	4025	4024	4021	4095	4093	4092	4091	179	17	175	174	180
	4014	4015	4016	4017	4018	4019	4020	4095	4144	4145	4193	4090	1	93	94	173
	4128	4183	4192	4101	4103	4098	4097	4096	4143	4146	4045	4089	2	125	95	96
	4129	4118	0[1]	4131	4133	4138	4140	4142	4147	4192	4046	4088	3	126	126	97
	4130	4117	4132	4130	4134	4139	4141	4148	4191	4048	4047	4087	4	127	123	100
	4113	4116	4129	4120	4135	4137	4149	4189	4190	4049	4050	4086	5	42	41	131
	4127	4121	4127	4126	4136	4150	4100	4083	4052	4052	4081	4085	6	0[1]	40	39
	4119	4122	4124	4125	4151	4183	4107	4084	4081	4053	4054	4083	7	33	34	33
·	4118	4123	4154	4153	4152	4184	4183	4085	4080	4056	4055	4084	8	32	35	29
·	4157	4155	4155	4170	4171	4182	4181	4066	4059	4057	4058	4082	9	31	30	27
·	4158	4159	4160	4169	4172	4179	4180	4067	4074	4075	4076	4081	10	15	29	28
32	4163	4162	4161	4168	4173	4178	4177	4068	4073	4072	4077	4080	11	14	17	16
	1	2	3 · · ·						· · · j · · ·						· · · 16	

[1] No sample. Refer to Appendix III for assumed uranium value.

APPENDIX III

TABLE OF URANIUM VALUES FOR SAMPLES

Uranium values (ppm) are arranged to correspond to the sample numbers and sites in Appendix II and Figure 8 respectively. To locate the uranium value for a sample number in Appendix II or a dot in Figure 8, read the i and j coordinate then locate the same i and j coordinate in the tables that follow.

1	90.0	4.5	1.3	1.4	2.8	.8	2.0	5.0	2.3	0.5	2.5	7.8	7.0	6.0	5.5	3.0
2	4.5	4.7	1.0	2.1	1.8	1.9	1.8	.6	2.5	4.5	5.0	1.6	3.5	2.0	.8	11.0
3	6.3	1.0	2.0	2.1	1.3	.4	1.5	2.8	2.3	9.3	1.5	.2	3.0	1.5	3.5	1.0
.	3.0	2.2	1.4	3.2	3.0	1.7	0.0	2.3	7.0	2.8	6.5	5.5	3.0	1.5	10.0	2.5
.	1.3	4.3	3.5	4.3	3.0	2.5	6.0	6.0	14.0	40.0	6.5	4.5	6.5	6.5	1.0	1.5
.	1.3	2.5	2.8	7.0	0.5	18.0	1.0	4.5	33.0	1.2	1.5	3.0	6.0	24.0	.3	2.0
	5.3	2.0	7.5	5.3	70.0	3.5	2.0	13.0	85.0	7.0	0.0	3.0	17.3	4.3	4.3	3.5
	2.8	3.8	3.3	6.0	12.0	3.0	19.0	18.0	13.0	2.0	23.0	6.5	3.5	2.2	10.0	2.5
	4.0	4.0	2.8	2.8	2.8	5.0	26.0	6.5	30.3	12.0	25.0	7.3	4.5	30.0	7.5	1.2
	3.0	2.5	2.5	5.5	4.0	2.9	20.0	19.3	1.3	3.5	15.0	4.0	6.3	8.5	1.5	1.7
	2.1	1.2	1.2	7.5	4.3	7.5	22.3	5.3	6.3	2.1	10.0	6.0	12.0	2.3	2.8	.3
	1.3	1.4	1.7	7.2	2.5	23.0	11.0	5.0	14.0	19.0	4.0	4.5	2.5	2.0	2.0	1.1
	3.5	2.5	2.1	1.8	15.0	21.0	28.3	3.5	11.0	15.0	20.0	4.5	4.3	1.5	1.0	1.9
	7.0	6.0	11.2	8.5	4.5	11.0	9.5	3.5	3.0	5.0	12.0	1.1	11.0	1.4	1.7	5.0
	3.3	6.5	11.3	8.0	2.8	7.0	1.7	5.0	25.0	35.0	4.5	9.0	6.0	6.8	7.0	1.3
	25.0	5.5	10.3	3.5	3.0	9.0	2.5	10.2	3.5	43.0	6.5	5.8	6.0	9.5	1.2	60.3
j	5.3	12.0	13.0	1.5	6.0	3.5	1.8	3.0	13.0	33.0	5.0	3.5	.5	.9	5.5	6.0
	20.0	2.3	5.3	1.5	3.3	7.0	21.2	2.2	2.0	5.5	2.5	4.0	.9	1.8	3.5	1.0
	1.7	5.3	7.1	9.0	1.3	13.0	7.3	2.3	3.5	9.5	2.4	3.3	1.8	3.4	2.0	2.3
	4.5	2.5	5.5	7.0	12.0	3.2	3.3	3.5	4.0	1.9	30.0	4.0	3.5	1.3	1.1	3.0
	5.3	4.0	45.3	5.3	49.3	33.0	3.0	3.3	1.4	3.9	2.1	2.8	2.8	2.0	5.5	1.4
	7.0	12.3	3.0	2.5	10.0	2.3	12.0	4.0	1.7	2.5	1.6	1.7	5.5	1.6	11.0	3.5
	2.5	2.5	4.0	1.2	10.0	6.0	15.0	10.3	8.3	2.3	1.5	1.5	2.0	1.3	300.3	3.3
	1.3	1.3	3.3	3.5	3.5	1.6	4.0	2.0	5.0	3.3	2.1	1.7	2.2	2.1	3.8	3.1
	3.0	3.2	5.5	4.5	6.3	5.0	28.0	7.3	3.5	35.0	23.0	2.5	1.5	2.3	2.3	2.3
	2.2	1.3	1.3	1.3	6.8	6.3	11.0	2.0	3.0	1.7	11.0	14.0	3.0	2.3	3.2	3.8
	4.3	1.3	2.3	4.3	5.0	10.8	1.6	19.0	2.5	10.0	4.3	165.3	2.3	1.3	1.3	4.2
	6.3	2.3	14.3	2.5	6.0	4.5	4.2	22.0	33.0	6.0	1.6	16.0	1.5	1.7	3.5	21.0
	4.3	8.3	5.3	13.3	5.0	6.0	23.3	15.3	9.0	1.8	2.4	6.5	1.7	3.0	4.8	23.3
	5.0	25.2	4.3	8.3	3.0	17.3	3.8	4.3	28.0	2.4	8.3	1.3	2.5	15.0	7.0	4.5
	11.8	7.3	5.8	11.3	1.2	5.3	4.3	6.2	5.8	1.2	8.8	6.5	1.7	2.5	8.3	2.3
32	2.3	8.3	7.3	22.0	11.0	3.3	7.3	4.3	4.3	3.3	1.7	2.5	4.3	3.5	2.5	5.3
	1	2	3 ...						... i ...							... 16

	17	18	19 ...						...i...							...32
1	1.0	.8	.3	.9	3.8	4.0	.5	.7	.5	1.4	.9	.7	.7	.4	.5	1.3
2	6.5	.7	1.1	5.5	.2	.2	.5	.7	.1	1.2	1.0	.9	1.2	1.4	.2	.2
3	1.5	3.5	1.0	.4	.1	.6	1.0	1.8	1.1	.9	1.4	.7	1.5	.3	.3	.6
.	1.1	1.1	1.1	2.5	2.0	3.5	.8	.9	.5	1.3	3.3	2.2	2.4	.4	.7	7.5
.	2.0	1.1	.8	2.4	.6	2.3	3.0	2.5	1.6	1.1	.9	1.3	1.0	.8	.4	4.8
.	4.5	1.2	1.7	1.2	3.5	1.2	1.6	6.0	1.1	1.5	1.9	.8	.6	.9	.4	1.2
	2.0	1.0	8.0	1.0	1.5	1.1	2.0	1.4	1.0	1.7	3.8	.3	1.3	1.1	1.2	.1
	10.0	1.0	1.1	2.8	1.2	1.7	6.5	1.7	1.1	3.0	1.4	1.4	.7	.3	1.7	1.1
	1.0	2.2	1.0	1.4	.8	1.2	1.4	1.6	1.1	.6	.3	.5	.2	.7	.7	.8
	2.0	2.5	.7	.9	2.5	.9	1.4	1.2	.8	.6	.7	.3	.2	.7	1.7	.9
	1.6	1.9	1.1	1.1	1.5	1.4	.5	.7	.8	.6	1.8	.1	1.1	.8	.1	1.7
	2.0	7.5	1.1	1.9	1.1	.9	1.0	1.3	1.2	1.7	1.2	2.0	2.0	.5	3.3	12.0
	10.0	3.0	3.0	2.5	1.6	5.5	.6	1.1	2.5	2.4	12.0	2.8	1.6	.5	1.8	4.5
.	2.0	1.0	1.6	1.4	.8	2.0	1.0	1.7	2.5	.7	.8	1.7	1.7	8.0	3.5	3.3
.	1.7	1.0	3.0	1.7	1.4	.4	.8	.9	3.0	5.0	1.5	2.0	1.6	9.0	2.9	1.3
i	5.7	5.3	4.5	1.9	2.5	2.5	1.2	1.0	2.2	1.0	.9	.8	2.3	1.3	1.4	.4
	60.0	30.0	8.5	1.5	3.0	1.6	1.8	2.5	2.1	2.3	1.3	1.6	.8	2.2	3.0	1.0
.	1.0	6.0	1.3	2.5	6.0	2.3	2.4	4.3	5.5	3.0	2.0	2.0	1.9	2.5	1.4	1.6
.	1.5	1.2	2.5	4.0	2.5	2.3	2.8	7.0	5.0	5.0	5.0	1.4	.9	1.0	1.6	2.0
	2.5	3.5	3.0	43.0	2.5	1.9	1.5	8.0	15.0	1.3	1.1	1.5	5.5	3.0	9.0	1.4
	2.0	1.4	2.3	3.5	1.9	10.0	2.0	16.0	12.0	4.5	1.1	3.0	1.3	5.5	3.5	1.4
	1.6	9.5	3.0	1.7	1.2	1.6	2.2	7.5	4.0	.8	1.5	6.5	1.6	1.3	1.5	5.0
	6.0	3.5	1.1	.8	1.0	.3	1.3	3.0	17.0	9.0	10.0	2.3	1.7	2.3	1.7	1.8
	2.2	5.0	2.5	6.3	2.0	2.2	2.3	1.3	2.2	1.4	2.5	6.5	4.5	5.0	.7	1.5
	[illegible]	100.0	12.0	10.0	2.8	4.5	3.0	1.7	2.1	2.5	7.0	10.0	2.1	.7	.3	.7
	5.0	15.0	38.0	16.0	7.5	1.3	1.4	1.3	1.3	2.3	2.5	.7	5.0	1.7	3.0	3.5
	4.0	52.0	52.0	15.0	1.3	1.4	.8	1.7	2.8	1.4	2.8	1.5	1.1	1.3	2.1	2.5
	17.0	30.0	2.0	3.5	5.0	2.5	3.3	.9	.7	1.6	6.0	1.4	3.8	3.0	1.9	1.2
	1.5	3.5	2.8	3.5	11.0	4.5	1.5	1.3	2.0	1.4	15.0	2.8	3.0	.7	1.0	2.3
.	1.3	1.3	3.3	6.0	1.1	3.3	1.5	8.0	90.0	9.0	15.0	13.0	2.3	.8	2.0	1.2
.	5.5	3.0	12.0	.7	6.5	1.6	1.0	3.8	6.0	6.0	1.5	2.3	2.1	.7	1.6	1.3
32	3.0	7.3	1.3	1.3	3.8	1.3	2.8	5.3	5.5	2.0	1.0	1.4	10.0	1.6	30.0	1.2

APPENDIX IV

OTHER PHASE MAPS

These phase maps are based on a combination of several peaks chosen from the power spectrum in Figure 9.

FIGURE IV-a. N-S set: P(-10,2)=3; P(-9,1)=3; P(-8,1)=3.

The crests of this combination of waves are still in a N-S direction but contain large areas of relative destruction or zones where waves are out of phase.

FIGURE IV-b. NE-SW set: P(5,5)=3; P(6,4)=3; P(7,3)=3.

The phase map produced from these peaks is somewhat distorted. The NE-SW crests are not continuous but oscillate along themselves and from one wave to the next.

FIGURE IV-c. NE-SW set: P(-4,4)=4; P(6,4)=3.

These two peaks were combined because they appeared to be mutually perpendicular. Their combination displays a pinching-out effect on the NE-SW crest lines of Figure 10d.

FIGURE IV-d. NE-SW-NW-SE set: P(-4,4)=4; P(6,4)=3; P(-9,1)=3.

The effect of adding the peak P(-9,1) to the previous set further pinches out some of

the NE-SW set of waves. It is obvious that modes of crests are beginning to form.

FIGURE IV-e. NE-SW-NW-SE set: P(-4,4)=4; P(6,4)=3; P(4,12)=4.

The combination of these peaks produces, what has been previously described as, an "egg box" pattern. This pattern is similar to the pattern shown in Figure 10-e.

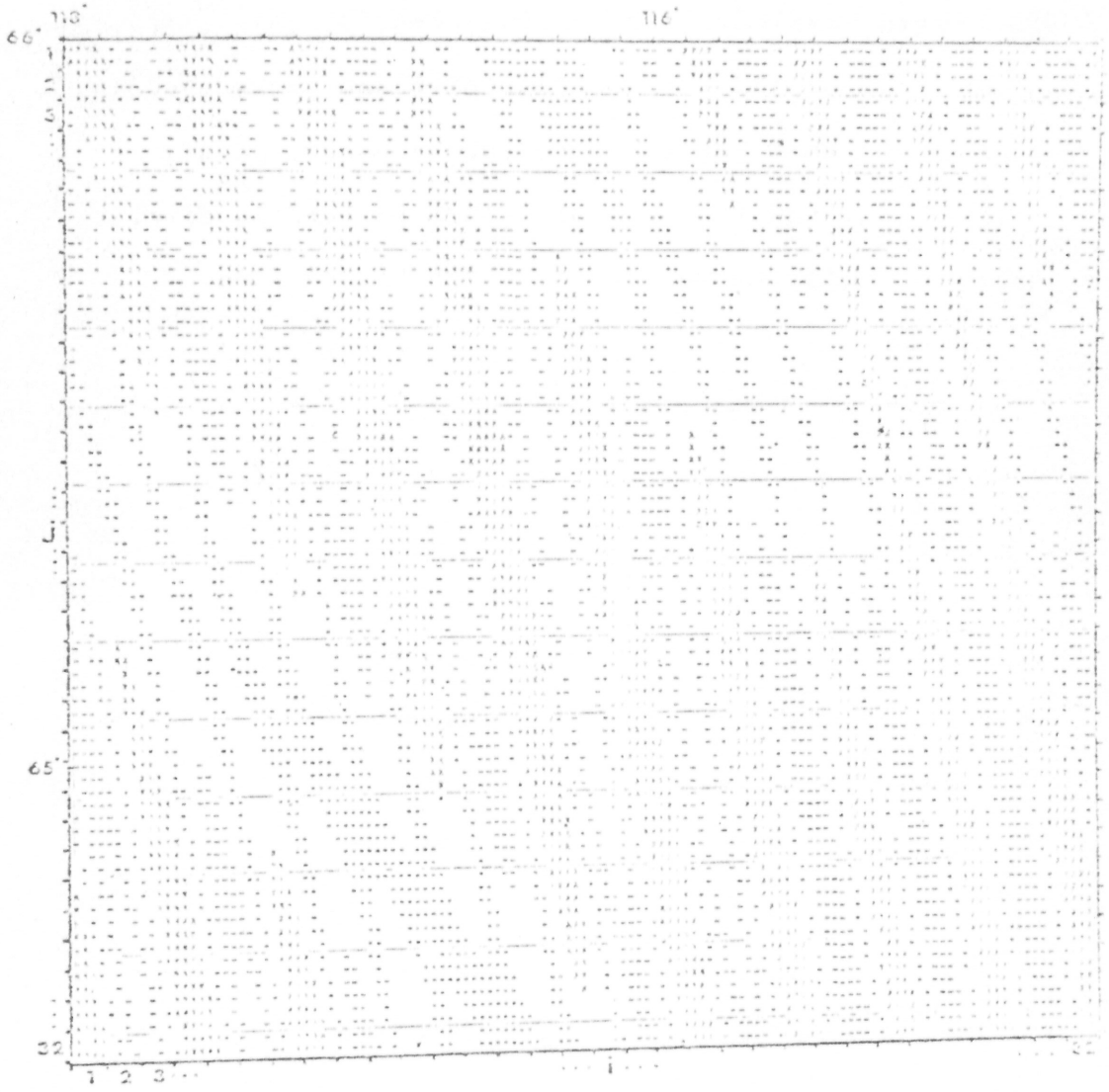

FIGURE IV-a. Phase map constructed from peaks P(-10,2), P(-9,1) and P(-8,1).

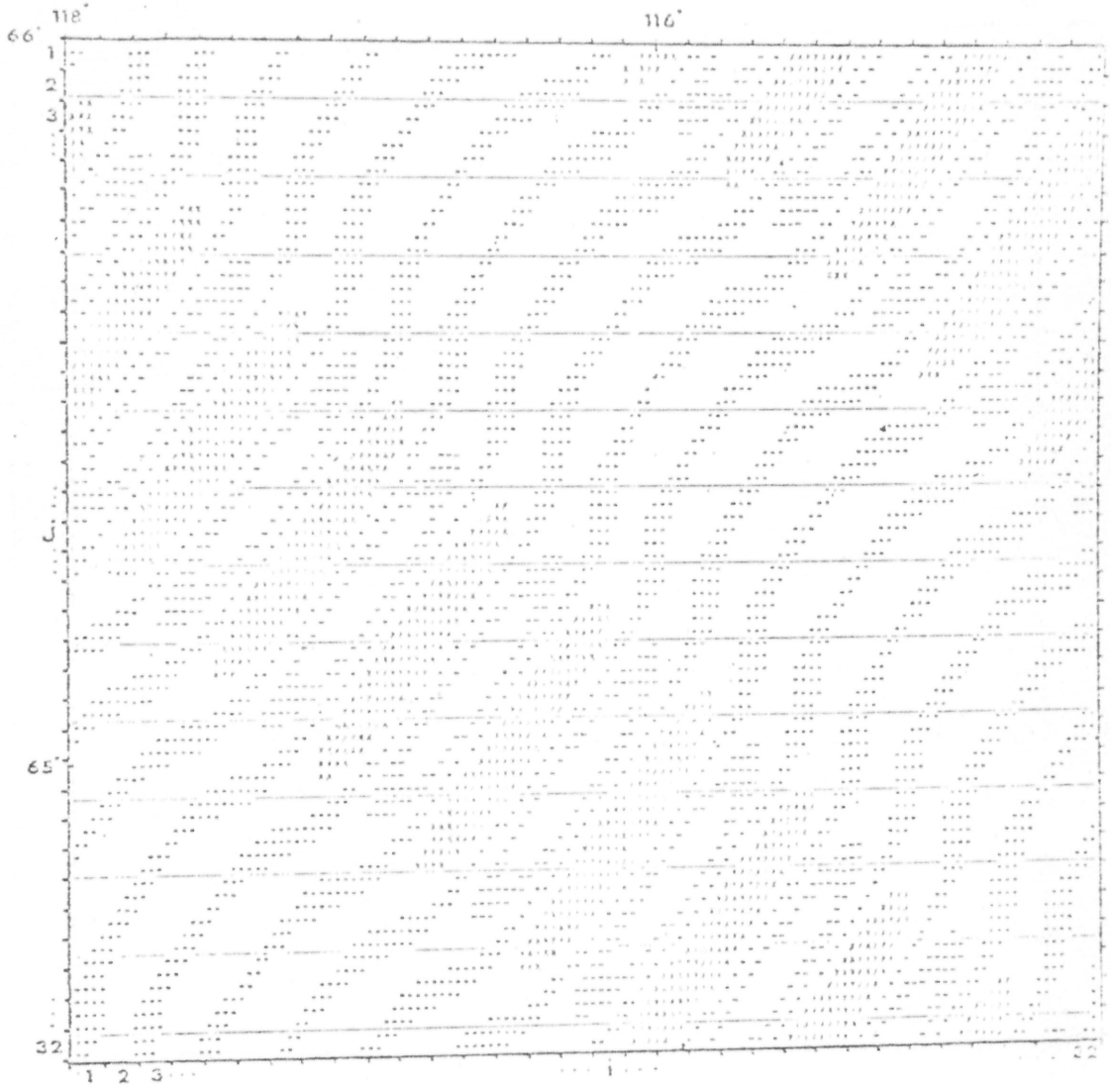

FIGURE IV-b. Phase map constructed from peaks P(5,5), P(6,4,) and P(7,3).

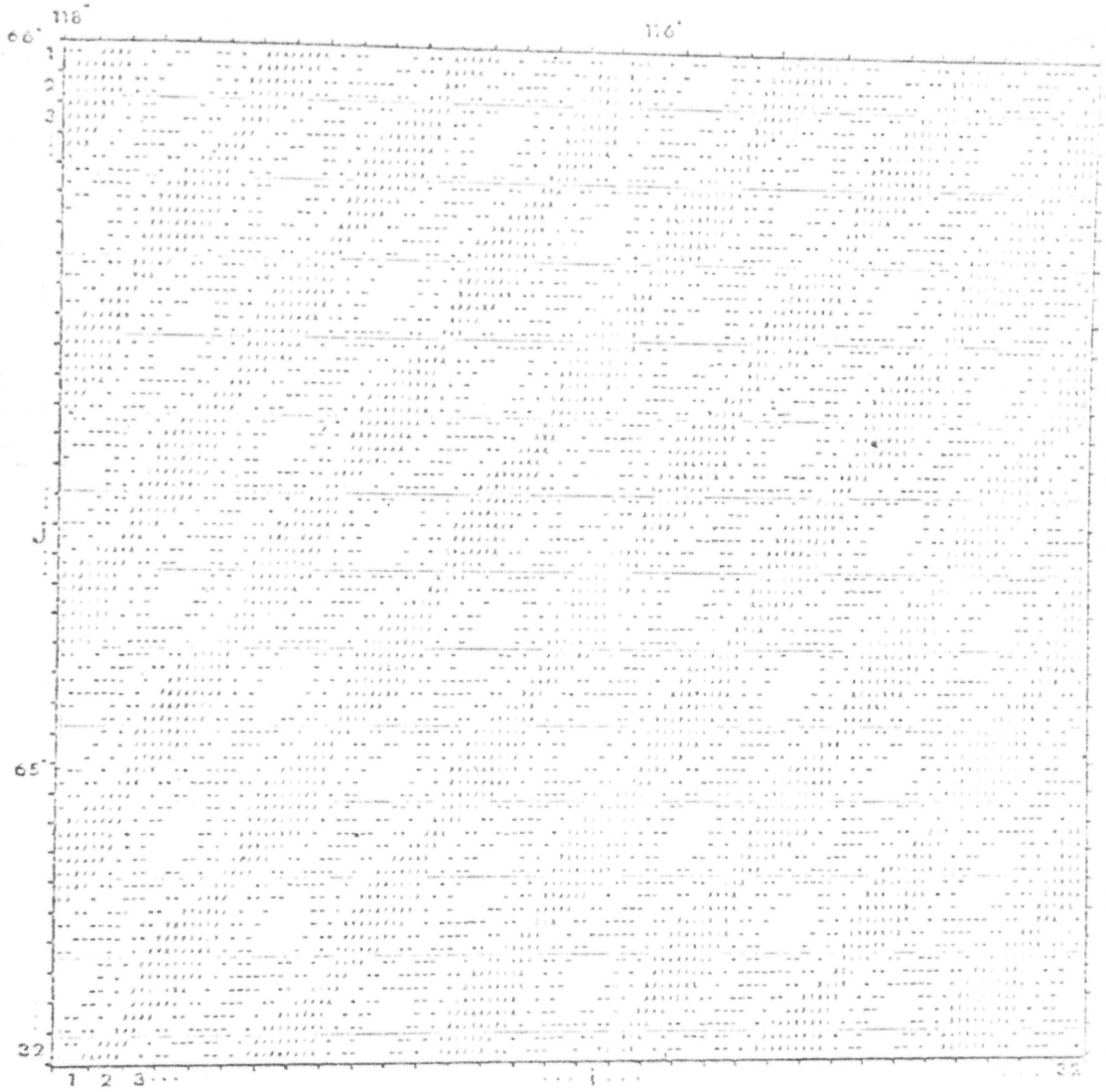

FIGURE IV-c. Pnase map constructed from peaks P(-4,4) and P(6,4).

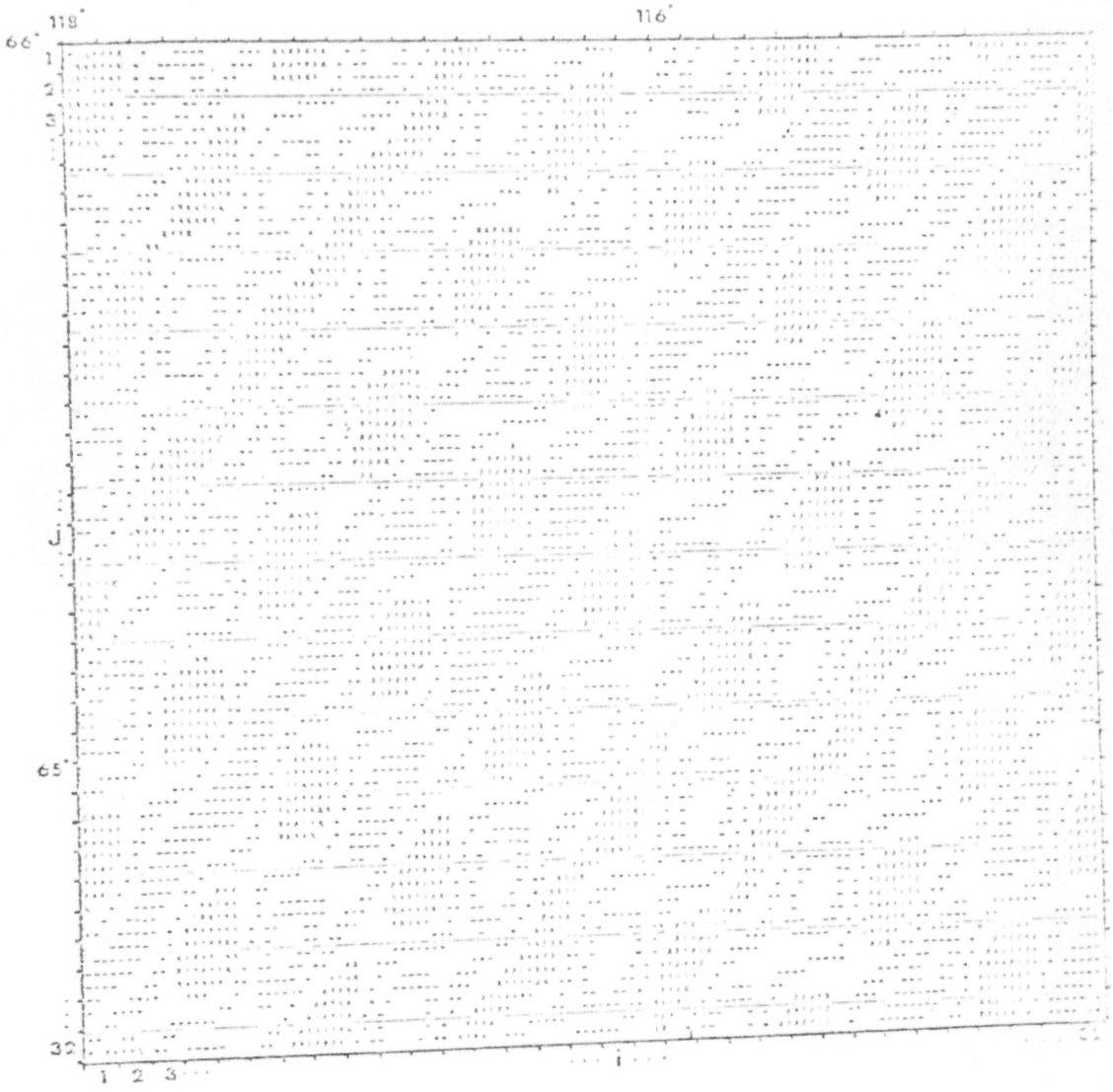

FIGURE IV-4. Phase map constructed from peaks P(-4,4), P(6,4) and P(-9,1).

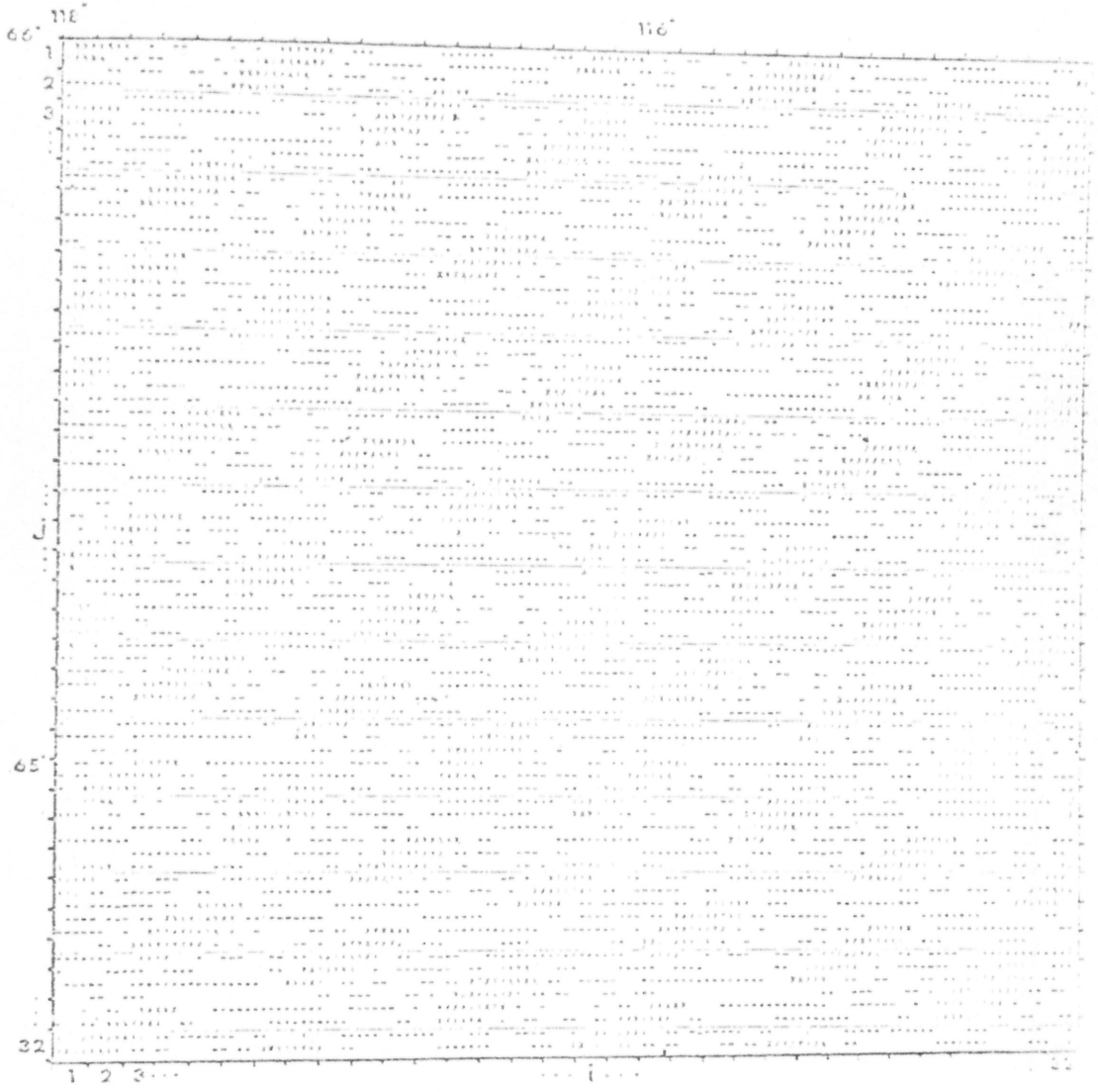

FIGURE IV-e. Phase map constructed from peaks P(-4,4), P(6,4) and P(4,12).